Cellular/Molecular

Orexin–Corticotropin-Releasing Factor Receptor Heteromers in the Ventral Tegmental Area as Targets for Cocaine

Gemma Navarro,[1]* César Quiroz,[2]* David Moreno-Delgado,[1]* Adam Sierakowiak,[2] Kimberly McDowell,[2] Estefanía Moreno,[1] William Rea,[2] Ning-Sheng Cai,[2] David Aguinaga,[1] Lesley A. Howell,[3] Felix Hausch,[4] Antonio Cortés,[1] Josefa Mallol,[1] Vicent Casadó,[1] Carme Lluís,[1] Enric I. Canela,[1][†] Sergi Ferré,[2][†] and Peter J. McCormick[1,3][†]

[1]Department of Biochemistry and Molecular Biology, Faculty of Biology, University of Barcelona, Center for Biomedical Research in Neurodegenerative Diseases Network and Institute of Biomedicine of the University of Barcelona, 08028 Barcelona, Spain, [2]Integrative Neurobiology Section, National Institute on Drug Abuse, Intramural Research Program, National Institutes of Health, Baltimore, Maryland 21224, [3]School of Pharmacy, University of East Anglia, Norwich, NR4 7TJ, United Kingdom, and [4]Max Planck Institute of Psychiatry, 80804 Munich, Germany

Release of the neuropeptides corticotropin-releasing factor (CRF) and orexin-A in the ventral tegmental area (VTA) play an important role in stress-induced cocaine-seeking behavior. We provide evidence for pharmacologically significant interactions between CRF and orexin-A that depend on oligomerization of CRF_1 receptor (CRF_1R) and orexin OX_1 receptors (OX_1R). $CRF_1R–OX_1R$ heteromers are the conduits of a negative crosstalk between orexin-A and CRF as demonstrated in transfected cells and rat VTA, in which they significantly modulate dendritic dopamine release. The cocaine target σ_1 receptor (σ_1R) also associates with the $CRF_1R–OX_1R$ heteromer. Cocaine binding to the $\sigma_1R–CRF_1R–OX_1R$ complex promotes a long-term disruption of the orexin-A–CRF negative crosstalk. Through this mechanism, cocaine sensitizes VTA cells to the excitatory effects of both CRF and orexin-A, thus providing a mechanism by which stress induces cocaine seeking.

Key words: cocaine; CRF receptor; GPCR heteromer; orexin receptor; sigma receptor

Introduction

The 41 aa neuropeptide corticotropin-releasing factor (CRF) plays an important role in stress-induced drug-seeking behavior (Sarnyai et al., 2001). This depends primarily on CRF release in the ventral tegmental area (VTA), which receives CRF inputs from the paraventricular nucleus and the limbic forebrain (Rodaros et al., 2007). Stress and addictive drugs sensitize VTA dopaminergic neurons to the effects of excitatory inputs by common synaptic modifications (Saal et al., 2003), which can be reproduced by VTA application of CRF (Ungless et al., 2003). In the

VTA of cocaine-experienced but not naive animals, stress-induced CRF release increases extracellular levels of glutamate and dopamine (Wang et al., 2005, 2007). Of the two known CRF receptors (CRF_1R and CRF_2R), CRF_1R is involved preferentially with stress-induced reinstatement of cocaine-seeking behavior and VTA dopamine release (Shaham et al., 1998; Lu et al., 2003; Lodge and Grace, 2005; Blacktop et al., 2011).

The 33- and 28-aa-long neuropeptides orexin-A (hypocretin-A) and orexin-B (hypocretin-B) are expressed within cell bodies in the lateral hypothalamus and adjacent perifornical area (Sakurai et al., 1998; de Lecea et al., 1998). These cells are the origin of an ascending arousal system that projects to the entire cortex, but apart from their well established role in arousal, orexins have a role in reward processes and substance-use disorders, which might depend on the dense orexinergic innervation of the dopaminergic cells of the VTA (Borgland et al., 2010; Mahler et al., 2014; Sakurai, 2014). A dichotomy in orexin function appears to be related to the two identified orexin receptors, with reward and arousal being associated closely with activation of OX_1R and OX_2R, respectively (Borgland et al., 2010; Mahler et al., 2014). The orexin–hypocretin system also drives cocaine reinstatement through activation of stress pathways, which includes the participation of CRF. Thus, central administration of orexin-A led to a dose-related reinstatement of cocaine seeking, which was prevented by a nonselective CRFR antagonist, and a selective OX_1R

antagonist blocked stress-induced reinstatement of previously extinguished cocaine-seeking behavior (Boutrel et al., 2005).

The same as for CRF, VTA is a key brain area involved in the ability of the orexinergic system to promote cocaine seeking. Intra-VTA administration of orexin-A reinstated cocaine self-administration, which was also associated with VTA glutamate and dopamine release (Wang et al., 2009). Intriguingly, although CRF and orexin-A are involved in stress-induced cocaine reinstatement by acting in the VTA, their mechanisms appeared independent (Wang et al., 2009). In the present study, we provide evidence for the existence of pharmacologically significant interactions between CRF and orexin-A that depend on CRF_1R–OX_1R oligomerization. CRF_1R–OX_1R heteromers are the conduits of a negative crosstalk between orexin-A and CRF observed in transfected cells and the VTA, in which they can significantly influence dendritic dopamine release. We also demonstrate that CRF_1R–OX_1R heteromers associate with σ_1 receptors (σ_1Rs) to form CRF_1R–OX_1R-σ_1R complexes and that cocaine binding to σ_1R in the complex promotes a long-term disruption of the orexin-A–CRF negative crosstalk. Through this mechanism, cocaine sensitizes VTA cells to the excitatory effects of both CRF and orexin-A.

Materials and Methods

Ligands and HIV transactivator of transcription-linked peptides. (−)-Cocaine HCl was purchased from Sigma and from the Spanish Agency of Medicine (number 2003C00220). σ_1R ligands PD144418 (1,2,3,6-tetrahydro-5-[3-(4-methylphenyl)-5-isoxazolyl]-1-propylpyridine oxalate) and PRE-084 2-(4-morpholinethyl) 1-phenylcyclohexanecarboxylate hydrochloride, CRF, orexins, SB334867 (*N*-(2-Methyl-6-benzoxazolyl)-*N*-1,5-naphthyridin-4-yl urea), and NBI27914 [5-chloro-*N*-(cyclopropylmethyl)-2-methyl-*N*-propyl-*N'*-(2,4,6-trichlorophenyl)-4,6-pyrimidinediamine hydrochloride] were purchased from Tocris Bioscience. To allow intracellular delivery, a peptide or protein can be fused to the cell-penetrating HIV transactivator of transcription (TAT) peptide (YGRKKRRQRRR; Schwarze et al., 1999). HIV TAT fused to a peptide with the amino acid sequence of a transmembrane domain (TM) of a GPCR can be inserted effectively into the plasma membrane as a result of both the penetration capacity of the TAT peptide and the hydrophobic property of the TM domain (He et al., 2011). HIV TAT-fused peptides with the amino acid sequences of OX_1R TM domains TM1, TM5, and TM7 were used (Genemad Synthesis). To obtain the right orientation of the inserted peptide, HIV TAT peptide was fused to the C terminus of OX_1R TM1, TM5, and TM7 peptides, with the following final amino acid sequences: WVLIAAYVAVFLIALVGNTLVYGRKKRRQRRR, SCFFFVTYLAPLGLMGMAYFQIFYGRKKRRQRRR, and YACFTFSHWLVYANSAANPIIYNFYGRKKRRQRRR, respectively.

Expression vectors, fusion proteins, and CRF_1R mutants. Sequences encoding amino acid residues 1-155 and 156-238 of yellow fluorescent protein (YFP) Venus protein were subcloned in pcDNA3.1 vector to obtain YFP Venus hemitruncated proteins. Human cDNAs for OX_1R, CRF_1R, ghrelin 1a receptors [growth hormone secretagogue 1a receptor ($GHS_{1a}R$)], or σ_1R, cloned into pcDNA3.1, were amplified without their stop codons using sense and antisense primers harboring the following: EcoRI and KpnI sites to clone CRF_1R, OX_1R, or $GHS_{1a}R$ in pcDNA3.1RLuc vector (p*RLuc*–N1; PerkinElmer Life and Analytical Sciences) or pEYFP–N1 vector (enhanced yellow variant of GFP; Clontech), HindIII and BamHI sites to clone σ_1R in pEYFP–N1 vector, or EcoRI and BamHI sites to clone CRF_1Rs and OX_1Rs in a Cherry containing vector (pcDNA3.1Cherry). Amplified fragments were subcloned to be in-frame with restriction sites of p*RLuc*–N1, pEYFP–N1, or pcDNA3.1Cherry vectors to provide plasmids that express proteins fused to *Renilla* Luciferase (RLuc), YFP, or Cherry on the C-terminal end (OX_1R–RLuc, CRF_1R–RLuc, OX_1R–YFP, CRF_1R–YFP, $GHS_{1a}R$–YFP, σ_1R–YFP, or CRF_1R–Cherry). Dr. Marian Castro (University of Santiago de Compostela, Santiago de Compostela, Spain) generously provided human β-arrestin 2–RLuc6 cDNA, cloned in pcDNA3.1 RLuc6 vector (pRLuc–N1; PerkinElmer Life and Analytical Sciences). For bimolecular fluorescence

complementation (BiFC) experiments, human cDNA for CRF_1R was also subcloned into pcDNA3.1–nVenus to provide a plasmid that expresses the receptor fused to the hemitruncated nYFP Venus on the C-terminal end of the receptor (CRF1R–nVenus), and human cDNA for OX_1R was also subcloned into pcDNA3.1–cVenus to provide a plasmid that expresses the receptor fused to the hemitruncated cYFP Venus on the C-terminal end of the receptor (OX_1R–cVenus). Two CRF_1R mutants were used: (1) CRF1R433, which lacks a large portion of the extracellular domain of the N terminus (amino acids 1–111) and is not able to bind ligands (Devigny et al., 2011); and (2) CRF1R432, with H405P and A119L mutations in the 3 IL that confer enhanced constitutive activity.

Cell clones, cell culture, and transient transfection. HEK-293T cells were grown in DMEM (Gibco) supplemented with 2 mM L-glutamine, 100 μg/ml sodium pyruvate, 100 U/ml penicillin/streptomycin, minimal essential medium non-essential amino acids solution (1:100), and 5% (v/v) heat-inactivated fetal bovine serum (Invitrogen) and were maintained at 37°C in an atmosphere with 5% CO_2. Cells were transiently transfected with the corresponding fusion protein cDNA by the polyethylenimine (Sigma) method. For receptor–heteromer signaling, 0.4 μg of OX_1R–RLuc cDNA and 0.3 μg of CRF_1R–YFP cDNA were transfected, which provides 80–90% of maximum bioluminescence resonance energy transfer (BRET), as deduced from the BRET saturation curves (Fig. 1), indicating a high degree of receptor heteromerization. For the expression of $GHS_{1a}R$–YFP, equal amounts of $GHS_{1a}R$–YFP and $GHS_{1b}R$ cDNA were transfected to ensure $GHS_{1a}R$ expression at the cell membrane. HEK-293T stable cell lines expressing CRF_1R–YFP or OX_1R–YFP fusion proteins were created by transfection of the corresponding cDNA in a pcDNA3.1 plasmid. Antibiotic-resistant clones were isolated with 1000 μg/ml geneticin (Invitrogen), and, after an appropriate number of passages, stable cell lines were selected and grown as above indicated in the presence of 500 μg/ml geneticin. Sample protein concentration was determined as a control of cell number using a Bradford assay kit (Bio-Rad) with bovine serum albumin (BSA) dilutions as standards.

Fluorescence complementation assays. HEK-293T cells were cotransfected with 0.6 μM CRF_1R–nVenus cDNA and 0.6 μM OX_1R–cVenus cDNA; 48 h after transfection, cells were treated or not with the indicated HIV TAT–TM-fused peptides (4 μM) for 60 min at 37°C. To quantify protein-reconstituted YFP Venus expression, cells (20 μg of protein) were distributed in 96-well microplates (black plates with a transparent bottom; Porvair), and fluorescence was read in a Fluo Star Optima Fluorimeter (BMG Labtech) equipped with a high-energy xenon flash lamp, using a 10 nm bandwidth excitation filter at 400 nm reading. Protein fluorescence expression was determined as fluorescence of the sample minus the fluorescence of cells not expressing the fusion proteins.

Resonance energy transfer experiments. For BRET assays, HEK-293T cells were transiently cotransfected with a constant amount of cDNA encoding for proteins fused to RLuc and with increasing amounts of the cDNA corresponding to proteins fused to YFP. To quantify protein YFP expression, cells (20 μg of protein) were distributed in 96-well microplates (black plates with a transparent bottom), and fluorescence was read in the Fluo Star Optima Fluorimeter using a 10 nm bandwidth excitation filter at 400 nm reading. Protein fluorescence expression was determined as fluorescence of the sample minus the fluorescence of cells expressing the BRET donor alone. For BRET measurements, the equivalent of 20 μg of cell suspension were distributed in 96-well microplates (Corning 3600, white plates; Sigma), and coelenterazine H (5 μM; Invitrogen) was added. After 1 min, readings were obtained using a Mithras LB 940 (Berthold Technologies) that allows the integration of the signals detected in the short-wavelength filter at 485 nm and the long-wavelength filter at 530 nm. To quantify protein RLuc expression luminescence, readings were also performed 10 min after addition of coelenterazine H (5 μM). For sequential resonance energy transfer (SRET) assays, HEK-293T cells were transiently cotransfected with constant amounts of cDNAs encoding for both receptor fused to RLuc and YFP proteins and with increasingly amounts of cDNA corresponding to the receptor fused to Cherry protein. After 48 h of transfection, quantifications were performed in parallel in aliquots of transfected cells (20 μg of protein): (1) quantification of receptor YFP or receptor RLuc expression was performed as indicated for BRET experiments; (2) for quanti-
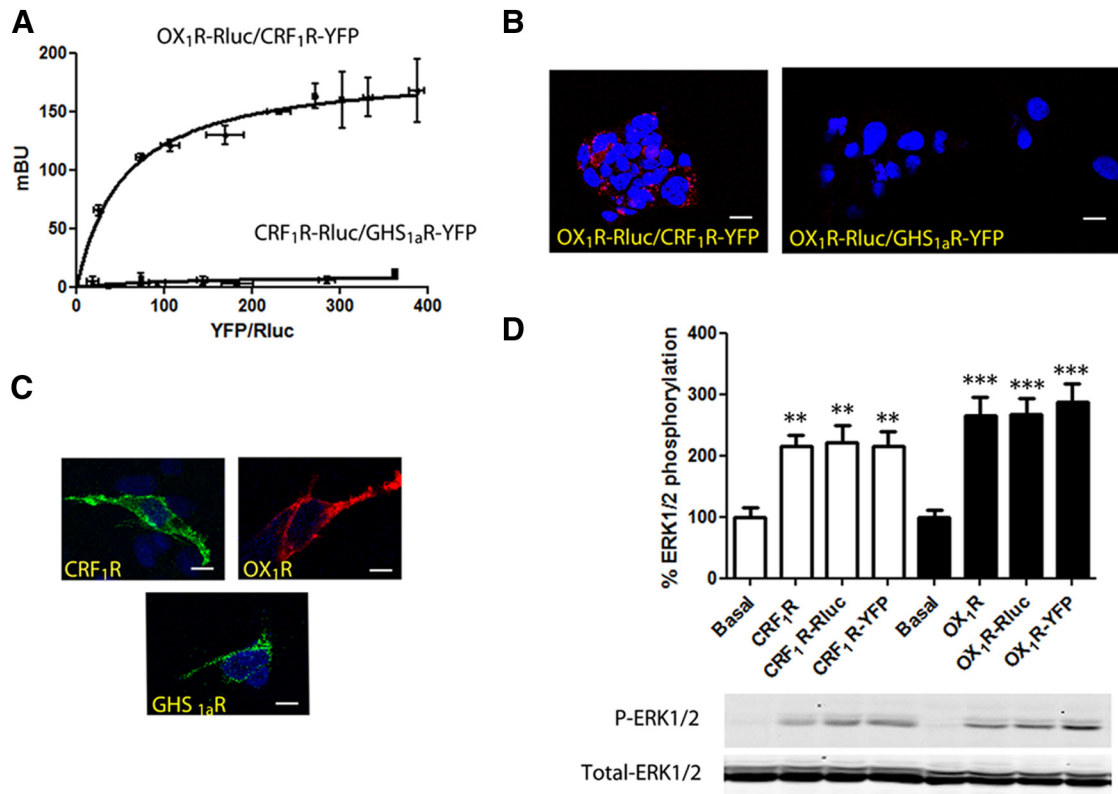
Figure 1. CRF$_1$R–OX$_1$R heteromers in transfected HEK-293T cells. **A**, BRET saturation experiments in cells transfected with OX$_1$R–RLuc cDNA (0.4 μg) and increasing amounts of CRF$_1$R–YFP cDNA (0.05– 0.5 μg). Low and linear BRET is observed in cells transfected with OX$_1$R–RLuc cDNA (0.4 μg) and GHS$_{1a}$R–YFP cDNA (0.4 –2 μg). BRET, expressed as mBU, is given as a function of 1000 $\times$ ratio of fluorescence of the acceptor (YFP) and Luciferase activity of the donor (Rluc). Values are means $\pm$ SEMs of six to seven replications of one independent experiment per point. **B**, Confocal microscopy images (superimposed sections) from PLA experiments performed in HEK-293T cells transfected with CRF$_1$R–YFP cDNA (0.3 μg) and OX$_1$R–RLuc cDNA (0.4 μg) (left) or GHS$_{1a}$R–YFP cDNA (2 μg) and OX$_1$R–RLuc cDNA (0.4 μg) (right). Heteromeric complexes appear as red spots and cell nuclei in blue (DAPI stained). Scale bars, 20 μm. **C**, Confocal microscopy images of HEK-293T cells transfected with CRF$_1$R–YFP cDNA (0.3 μg; left), OX$_1$R–RLuc cDNA (0.4 μg; middle), or GSH$_{1a}$R–YFP (2 μg; right). YFP-fused receptors are identified by their own fluorescence (green) and OX$_1$R–RLuc by immunocytochemistry (red). Scale bars, 10 μm. **D**, ERK1/2 phosphorylation in HEK-293T cells transfected with CRF$_1$R, CRF$_1$R–RLuc, or CRF$_1$R–YFP cDNA (0.3 μg; white columns) or with OX$_1$R, OX$_1$R–RLuc, or OX$_1$R–YFP cDNA (0.4 μg; black columns) were treated with CRF (100 nM) or orexin-A (50 nM), respectively. Values are means $\pm$ SEMs of seven experiments per group and are expressed as percentage of basal levels (100%). One-way ANOVA followed by Bonferroni's multiple comparison *post hoc* test shows significant agonist effect versus basal values (**$p < 0.01$ and ***$p < 0.001$). Representative Western blots are at the bottom.

fication of receptor Cherry expression, cells were distributed in 96-well microplates (Corning black plates with a transparent bottom), and fluorescence was read in the Fluo Star Optima Fluorimeter using a 10 nm bandwidth excitation filter at 590-nm reading; and (3) for quantification of SRET, cells were distributed in 96-well microplates (black plates with a transparent bottom), and coelenterazine H (5 μM) was added. After 1 min, the readings were collected using a using a Fluo Star Optima Fluorimeter that allows the integration of the signals detected in the short-wavelength filter at 530 nm and the long-wavelength filter at 590 nm. Net BRET and net SRET were defined as [(long-wavelength emission)/(short-wavelength emission)] − Cf, where Cf corresponds to [(long-wavelength emission)/(short-wavelength emission)] for the donor construct expressed alone in the same experiment. Both fluorescence and luminescence of each sample were measured before every experiment to confirm similar donor expressions (~100,000 bioluminescence units) while monitoring the increase in acceptor expression (1000–40,000 fluorescence units). BRET or SRET was expressed as milliBRET (mBU) or milliSRET (mSU) units (net BRET or SRET $\times$ 1000). Data were fitted to a nonlinear regression equation, assuming a single-phase saturation curve with GraphPad Prism software (GraphPad Software). The relative amount of BRET or SRET is given as a function of 100 $\times$ the ratio between the fluorescence of the acceptor (YFP or Cherry) and the Luciferase activity of the donor (RLuc).

Proximity ligation assay. For proximity ligation assays (PLAs), transfected cells were grown on glass coverslips and were fixed in 4% paraformaldehyde for 15 min, washed with PBS containing 20 mM glycine, permeabilized with the same buffer containing 0.05% Triton X-100, and

washed successively with PBS. Heteromers were detected using the Duolink II *in situ* PLA detection Kit (OLink Bioscience) following the instructions of the supplier. To detect both OX$_1$R–RLuc–CRF$_1$R–YFP and OX$_1$R–RLuc–GHS$_{1a}$R–YFP heteromers, a mixture of equal amounts of rabbit anti-RLuc antibody (EMD Millipore) and mouse anti-YFP antibody (Santa Cruz Biotechnology) was used and incubated with anti-rabbit plus and anti-mouse minus PLA probes. Cells were mounted using the mounting medium with DAPI. The samples were observed in a Leica SP2 confocal microscope equipped with an apochromatic 63$\times$ oil-immersion objective (numerical aperture 1.4) and 405 and 561 nm laser lines. For each field of view, a stack of two channels (one per staining) and 9–15 Z stacks with a step size of 1 μm were acquired. Images were opened and processed with NIH Image J confocal.

Immunocytochemistry. Cells were fixed in 4% paraformaldehyde for 15 min and washed with PBS containing 20 mM glycine (buffer A) to quench the aldehyde groups. After permeabilization with buffer A containing 0.2% Triton X-100 for 5 min, cells were treated with PBS containing 1% BSA. After 1 h at room temperature, cells were labeled with the primary mouse monoclonal anti-RLuc receptor antibody (1:200; Millipore) for 1 h to detect OX$_1$R–RLuc, washed, and stained with the secondary Cy3 donkey anti-mouse antibody (1:200; Jackson ImmunoResearch). CRF$_1$R fused to YFP protein were detected by their fluorescence properties. The samples were rinsed several times and mounted with a medium suitable for immunofluorescence (30% Mowiol; Calbiochem). Samples were observed in a Leica SP2 confocal microscope.

Rat VTA slices. Male Sprague Dawley rats (2 months old; animal facility of the Faculty of Biology, University of Barcelona) were used. The

animals were housed two per cage and kept on a 12 h dark/light cycle with food and water available *ad libitum*, and experiments were performed during the light cycle. All procedures were approved by the Catalan Ethical Committee for Animal Use (CEAA/DMAH 4049 and 5664). Animals were killed by decapitation under 4% isoflurane anesthesia, and brains were rapidly removed, placed in ice-cold oxygenated (O_2/CO_2, 95%/5%) Krebs–HCO_3^- buffer (in mM: 124 NaCl, 4 KCl, 1.25 KH_2PO_4, 1.5 $MgCl_2$, 1.5 $CaCl_2$, 10 glucose, and 26 $NaHCO_3$, pH 7.4), and sliced at 4°C using a brain matrix (Zivic Instruments). VTA slices (500 μm thick) were kept at 4°C in Krebs–HCO_3^- buffer during the dissection; each slice was transferred into a 12-well plate with Corning Netwell inserts, containing 2 ml of ice-cold Krebs–HCO_3^- buffer. The temperature was raised to 23°C, and, after 30 min, the medium was replaced by 2 ml of fresh Krebs–HCO_3^- buffer (23°C). Slices were incubated under constant oxygenation (O_2/CO_2, 95%/5%) at 30°C for 4 h in an Eppendorf Thermomixer (5 Prime), and the medium was replaced by fresh Krebs–HCO_3^- buffer and incubated for 30 min before the addition of any agent. After incubation, the solution was discarded, and slices were frozen on dry ice and stored at −80°C until ERK1/2 phosphorylation was determined.

Akt and ERK1/2 phosphorylation. Cells or rat VTA slices were treated or not with the indicated ligands for the indicated time and were lysed by the addition of 300 μl of ice-cold lysis buffer (50 mM Tris-HCl, pH 7.4, 50 mM NaF, 150 mM NaCl, 45 mM β-glycerophosphate, 1% Triton X-100, 20 μM phenyl-arsine oxide, 0.4 mM NaVO$_4$, and protease inhibitor mixture). Cellular debris was removed by centrifugation at 13,000 × g for 5 min at 4°C, and the protein was quantified by the bicinchoninic acid method using BSA dilutions as standard. Akt or ERK1/2 phosphorylation was then determined by Western blot as described previously (Moreno et al., 2014), using a rabbit anti-phospho-Ser473 Akt antibody (1:2500; Signalway Antibody) for Akt phosphorylation or mouse anti-phospho-ERK1/2 antibody (1:2500; Sigma) and rabbit anti-ERK1/2 antibody that recognizes both phosphorylated and nonphosphorylated ERK1/2 (1:40,000; Sigma).

β-Arrestin 2 recruitment. Arrestin recruitment was determined as described previously (Moreno et al., 2014). Briefly, BRET experiments were performed in HEK-293T cells 48 h after transfection with the cDNA corresponding to the indicated receptors fused or not to the YFP and β-arrestin 2–RLuc cDNA (0.5 μg). Cells (20 μg protein) were distributed in 96-well microplates (Corning 3600, white plates with white bottom; Sigma) and were incubated with the indicated antagonist for 10 min and stimulated with the agonist for 10 min before the addition of coelenterazine H (5 μM; Invitrogen). After 1 min of adding coelenterazine H, BRET between β-arrestin 2–RLuc and receptor YFP was determined and quantified as described above.

cAMP production. Transfected HEK-293T cells were incubated in serum-free medium for 16 h before the experiment. Cells were preincubated for 15 min at 37°C with zardaverine (50 μM; Tocris Bioscience) and treated for 15 min with the indicated concentration of agonists in the presence or absence of forskolin (0.5 μM; Sigma). When indicated, receptor antagonists were preincubated 10 min before agonist addition. To stop the reaction, cells were placed on ice, washed with ice-cold PBS, and centrifuged at 2500 × g for 5 min at 4°C. The pellet was washed with ice-cold HBSS with 10 mM glucose and resuspended with 200 μl of $HClO_4$ (4%) for 30 min, and 1.5 M KOH was added to reach neutral pH. Samples were centrifuged at 15,000 × g for 30 min at 4°C, and the supernatant was frozen at −20°C. Accumulation of cAMP was measured with Cyclic AMP (^{3}H) Assay System (GE Healthcare) as described by the manufacturer.

Dynamic mass redistribution assays. Dynamic mass redistribution (DMR) was determined using an EnSpire Multimode Plate Reader (PerkinElmer Life and Analytical Sciences). Refractive waveguide grating optical biosensors, integrated in 384-well microplates, allow extremely sensitive measurements of changes in local optical density in a detecting zone up to 150 nm above the surface of the sensor. Cellular mass movements induced during receptor activation were detected by illuminating the underside of the biosensor with polychromatic light and measured as changes in wavelength of the reflected monochromatic light that is a sensitive function of the index of refraction. The magnitude of this wavelength shift (in picometers) is directly proportional to the amount of DMR. Briefly, 24 h before the assay, cells were seeded at a density of 5000 cells per well in 384-well sensor microplates with 30 μl of growth medium and cultured for 24 h (37°C, 5% CO_2) to obtain 70–80% confluent monolayers. Cells were washed twice with assay buffer (HBSS with 20 mM HEPES, pH 7.15) and incubated 2 h in 40 μl/well assay buffer with 0.1% DMSO at 24°C, the sensor plate was scanned, and a baseline optical signature was recorded before incubating the indicated antagonists for 30 min and adding 10 μl of agonist dissolved in assay buffer containing 0.1% DMSO. DMR responses were monitored for at least 8000 s. Kinetic results were analyzed using EnSpire Workstation Software version 4.10 (EnSpire Software), and curves were normalized with respect to the baseline.

In vivo VTA dendritic dopamine release. Male Sprague Dawley rats (3 months old; Charles River Laboratories) were used. Animals were housed two per cage and kept on a 12 h dark/light cycle with food and water available *ad libitum*. Experiments were performed during the light cycle. All animals used in the study were maintained in accordance with the guidelines of National Institutes of Health animal care, and the animal research conducted to perform this study was reviewed and approved by the National Institute on Drug Abuse Intramural Research Program Animal Care and Use Committee (Protocol 12-BNRB-73). Rats were deeply anesthetized with 3 ml/kg Equithesin [4.44 g of chloral hydrate, 0.972 g of Na pentobarbital, 2.124 g of $MgSO_4$, 44.4 ml of propylene glycol, 12 ml of ethanol, and distilled H_2O up to 100 ml of final solution (National Institute on Drug Abuse Pharmacy)] and implanted unilaterally in the VTA (coordinates in mm from bregma with a 10° angle in the coronal plane: anterior, 5.6; lateral, 2.4; vertical, 9) with a specially designed microdialysis probe that allows the direct infusion of large peptides within the sampling area. After surgery, rats were allowed to recover in hemispherical CMA-120 cages (CMA Microdialysis) equipped with two-channel overhead fluid swivels (Instech) connected to a sample collector (CMA 470; CMA). Twenty-four hours after implanting the probe, in the middle of the light period of the light/dark cycle, experiments were performed on freely moving rats in the same hemispherical home cages in which they recovered overnight from surgery. An ACSF (in mM: 144 NaCl, 4.8 KCl, 1.7 $CaCl_2$, and 1.2 $MgCl_2$) was pumped through the probe at a constant rate of 1 μl/min. After a washout period of 90 min, dialysate samples were collected at 20 min intervals. For peptide infusion, orexins and CRF were dissolved in ACSF to a final concentration of 10 μM, whereas HIV TAT-fused peptides were dissolved in 0.1% DMSO in ACSF to a final concentration of 30 μM (TM1 and TM5) or 60 μM (TM7). All peptides were injected with a 1 μl syringe (Hamilton) driven by an infusion pump and coupled with silica tubing (73 μm inner diameter; Polymicro) to the microdialysis probe infusion port (dead volume, 40 nl), which was primed with ACSF and plugged during implantation. All peptides were delivered at a rate of 16.6 nl/min. The OX_1R antagonist SB334667 was dissolved in sterile saline and administered intraperitoneally (10 mg/kg) 40 min before peptide infusion. The CRF_1R antagonist NBI27914 was dissolved in 5% DMSO in water and administered intraperitoneally (10 mg/kg) 40 min before peptide infusion. The σ_1R agonist PRE-084 was dissolved in ACSF at a concentration of 100 μM and was perfused through the microdialysis probe (reverse dialysis). Cocaine HCl was administered intraperitoneally 24 h before the start of the microdialysis experiment at a dose of 15 mg/kg. At the end of the experiment, rats were given an overdose of Equithesin, the brains were extracted and fixed in formaldehyde, and probe placement was verified using cresyl violet staining. Dopamine content was measured by HPLC coupled with a coulometric detector (5200a Coulochem III; ESA).

Statistics. Sample sizes were between 5 and 10, which our previous published work indicated are sufficient to perform appropriate statistical analysis. Parametric statistics (unpaired *t* test and one-way or repeated-measures ANOVA) were used, because the different groups analyzed showed normality and homogeneity of variance. GraphPad Prism software version 5 was used for the statistical analysis.

Results

Expression and functional characterization of heteromers between OX_1R and CRF_1R in transfected cells

BRET and PLA experiments were performed in HEK-293T cells transfected with OX_1R–RLuc and CRF_1R–YFP (Figs. 1*A*,*B*).
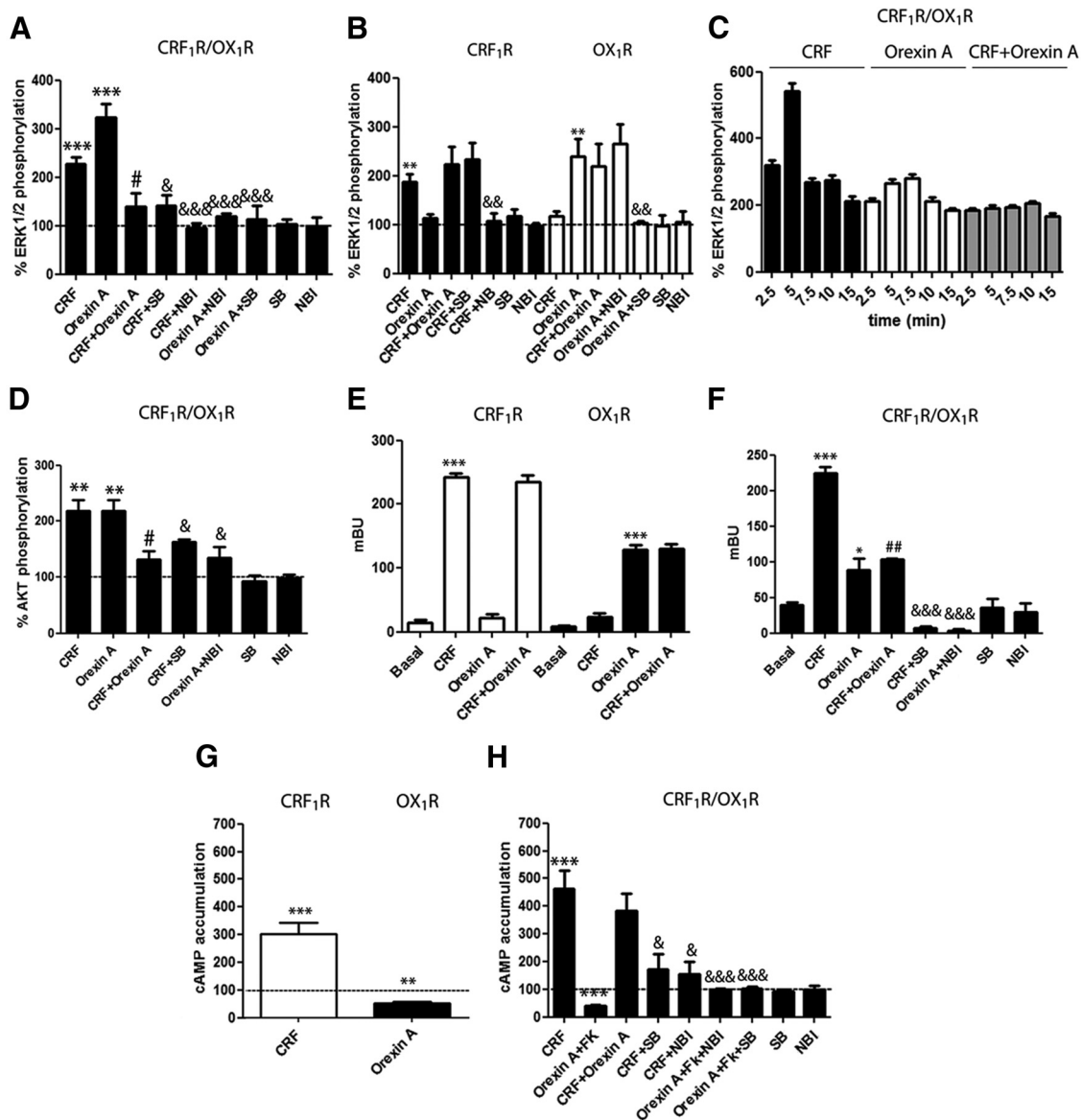
Figure 2. CRF₁R–OX₁R heteromer function in transfected HEK-293T cells. *A–C*, ERK1/2 phosphorylation was performed in cells transfected with CRF₁R–YFP cDNA (0.3 μg; *B*) or OX₁R–RLuc cDNA (0.4 μg; *B*) or both (*A, C*) pretreated (10 min) with vehicle, the OX₁R antagonist SB334667 (SB; 1 μM), or the CRF₁R antagonist NBI27914 (NBI; 1 μM), followed by treatment with medium, CRF (100 nM), orexin-A (50 nM), or both for 7 min (*A, B*) or for 2.5, 5, 7.5, 19, and 15 min (*C*). Values are means $\pm$ SEMs of five to six experiments per group and are expressed as percentage of basal levels (100%; dotted line). *D*, Akt phosphorylation was determined in cells transfected with CRF₁R–YFP cDNA (0.3 μg) and OX₁R–RLuc cDNA (0.4 μg), pretreated (10 min) with vehicle, the OX₁R antagonist SB334667 (SB; 1 μM), or the CRF₁R antagonist NBI27914 (NBI; 1 μM), followed by treatment (7 min) with medium, CRF (100 nM), orexin-A (50 nM), or both. Values are means $\pm$ SEMs of six to eight experiments per treatment and are expressed as percentage of basal levels (100%; dotted line). *E, F*, β-Arrestin 2 recruitment measured by BRET in cells transfected with CRF₁R–YFP cDNA (0.3 μg; *E*, white bars) or OX₁R–YFP cDNA (0.4 μg; *E*, black bars), or both (*F*) and β-arrestin 2–RLuc cDNA (0.5 μg). Cells were pretreated (10 min) with vehicle, SB334667 (SB; 1 μM), or NBI27914 (NBI; 1 μM), followed by treatment (7 min) with CRF (100 nM), orexin-A (50 nM), or both. Values are means $\pm$ SEMs of five to six experiments per treatment. *G, H*, cAMP accumulation was determined in cells transfected with CRF₁R–YFP cDNA (0.3 μg; *G*, white bar) or OX₁R–RLuc cDNA (0.4 μg; *G*, black bar), or both (*H*). Cells were pretreated (10 min) with vehicle, the OX₁R antagonist SB334667 (SB; 1 μM), or the CRF₁R antagonist NBI27914 (NBI; 1 μM), followed by treatment (7 min) with medium, CRF (100 nM), orexin-A (50 nM), or both. Values are means $\pm$ SEMs of six to eight experiments per treatment and expressed as increases of basal levels or as decreases of forskolin-induced cAMP accumulation (for orexin-A; 100%; dotted line). In *A, B, D–F*, and *H*, One-way ANOVA followed by Bonferroni's multiple comparison *post hoc* test shows significant single agonist effect versus basal values (*$p < 0.05$, **$p < 0.01$, and ***$p < 0.001$), or CRF plus orexin-A treatment versus CRF or orexin-A treatment (#$p < 0.05$) or antagonist plus agonist versus agonist with or without forskolin (FK; &$p < 0.05$, &&$p < 0.01$, and &&&$p < 0.001$). In *G*, unpaired Student's *t* test (two-tailed) shows significant difference of single agonist treatment versus basal values (**$p < 0.01$ and ***$p < 0.001$).

These fusion proteins properly trafficked to the cell membrane, as shown by confocal microscopy (Fig. 1*C*), and were functional, as shown by comparing their ability to increase ERK1/2 phosphorylation with that of native receptors (Fig. 1*D*). BRET saturation curves were obtained in cells expressing OX₁R–RLuc and increasing amounts of CRF₁R–YFP (Fig. 1*A*), with BRET_max of 186 ± 6 mBU and BRET₅₀ of 54 ± 7, indicating that these receptors can indeed form heteromers. As a negative control, a low and

linear BRET was detected in cells expressing CRF₁R–RLuc and increasing amounts of GHS₁ₐR fused to YFP (Fig. 1*A*). Accordingly, receptor heteromers were also visualized as red spots by using PLA in cells expressing OX₁R–RLuc and CRF₁R–YFP but not in cells expressing CRF₁R–RLuc and GHSR₁ₐ–YFP (Fig. 1*B*).

CRF or the OX₁R agonist orexin-A induced ERK1/2 phosphorylation in cells coexpressing CRF₁R and OX₁R (Fig. 2*A*). Orexin-A-induced signaling was inhibited by the OX₁R antago-

nist SB334867 and the CRF_1R antagonist NBI27914, that did not modify basal levels by themselves, and vice versa, CRF-induced ERK1/2 phosphorylation was antagonized by both NBI27914 and SB334667. Thus, CRF_1R–OX_1R heteromers display cross-antagonism, a property seen in previous receptor heteromers (Guitart et al., 2014; Moreno et al., 2014). A negative crosstalk was also observed because ERK1/2 phosphorylation during coactivation of both receptors was significantly lower compared with that induced by single activation of either CRF_1R or OX_1R (Fig. 2A). Cross-antagonism and negative crosstalk were not attributable to either the lack of ligand specificity, because they were not observed in cells expressing single receptors (Fig. 2B), or a change in the shape of the time–response curve of ERK1/2 phosphorylation (Fig. 2C). Negative crosstalk and cross-antagonism were also observed at the level of Akt phosphorylation (Fig. 2D). β-Arrestin recruitment was also analyzed, because it has been shown to mediate ERK1/2 and Akt phosphorylation for several GPCRs (Kovacs et al., 2009). Orexin-A but not CRF significantly increased control BRET values in cells expressing β-arrestin 2–RLuc and OX_1R–YFP. Similarly, CRF but not orexin-A increased BRET values in cells expressing β-arrestin 2–RLuc and CRF_1R–YFP (Fig. 2E), indicating both the specificity of the ligands and the ability of these receptors to recruit β-arrestin 2 when activated. Significantly, not only CRF but also orexin-A significantly increased BRET values in cells expressing β-arrestin 2–RLuc, CRF_1R–YFP, and OX_1R (Fig. 2F). During coactivation with both agonists CRF and orexin-A, a negative crosstalk was observed at the level of β-arrestin 2 recruitment. Furthermore, cross-antagonism could also be demonstrated, and CRF-promoted and orexin-A-promoted β-arrestin 2 recruitment were counteracted by SB334867 and NBI27914, respectively (Fig. 2F).

Orexin-A decreased forskolin-stimulated cAMP in cells expressing OX_1R, indicating receptor coupling to a G_i-protein, and CRF promoted an increase in cAMP production in cells expressing CRF_1R, indicating receptor coupling to a G_s-protein (Fig. 2G). The same findings were observed in cells coexpressing OX_1R and CRF_1R, suggesting that the receptors can signal independently through their preferred G-proteins in the CRF_1R–OX_1R heteromer (Fig. 2H). Cross-antagonism could also be observed at the adenylyl-cyclase level in cells coexpressing OX_1R and CRF_1R. Thus, orexin-A-induced inhibition of forskolin-stimulated cAMP accumulation was counteracted not only by the OX_1R antagonist SB334867 but also by the CRF_1R antagonist NBI27914. Equally, CRF-induced cAMP accumulation was counteracted by both NBI27914 and
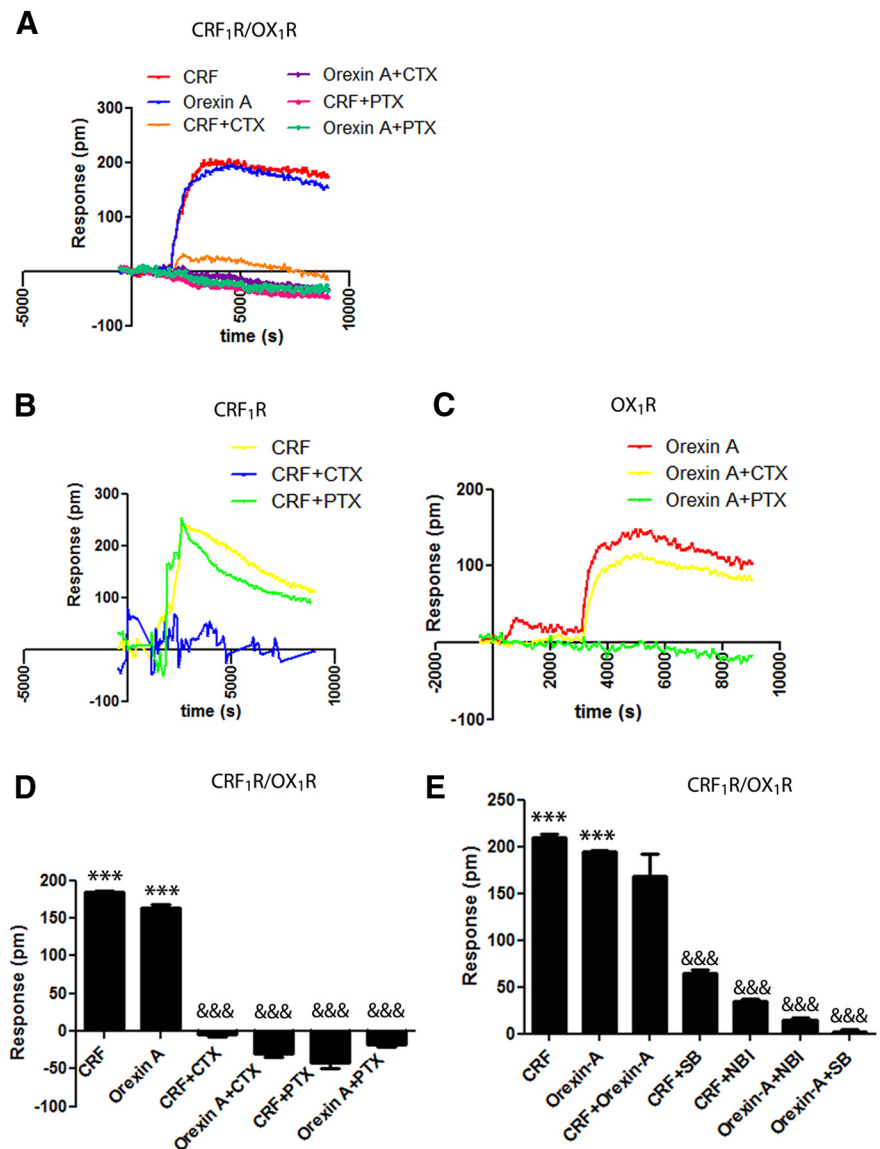
Figure 3. CRF_1R–OX_1R heteromer signaling detected by DMR. DMR was determined in HEK-293T cells stably transfected with OX_1R and transiently transfected with CRF_1R cDNA (0.3 μg; **A, D, E**) or only stably transfected with OX_1R (**C**) or transiently transfected with CRF_1R cDNA (0.3 μg; **B**). Cells were pretreated (overnight) with (**A–D**) vehicle, PTX (10 ng/ml), or CTX (100 ng/ml) or vehicle, the OX_1R antagonist SB334667 (SB; 1 μM) or the CRF_1R antagonist NB127914 (NBI; 1 μM), followed by treatment (7 min) with CRF (100 nM), orexin-A (50 nM), or both (**E**). **A–C**, Representative picometer shifts of reflected light wavelength (picometers) versus time; each curve shows the mean of a representative optical trace experiment performed in triplicate. **D, E**, Maximum responses are derived from the resulting picometer shifts of reflected light wavelength (picometers) versus time curves. Values are means $\pm$ SEMs of four to five experiments per group. One-way ANOVA followed by Bonferroni's multiple comparison post hoc tests show significant agonist effect versus basal values (***$p < 0.001$), no significant effect of CRF plus orexin-A treatment versus CRF or orexin-A treatment, and significant effect of agonist plus antagonist or toxin treatment versus agonist alone ($^{\&\&\&}p < 0.001$).

SB334867 (Fig. 2H). A canonical G_s–G_i interaction at the adenylyl-cyclase level could not be observed during coactivation of both receptors with CRF and orexin-A, showing cAMP accumulation similar to that obtained with CRF alone (Fig. 2H). This would indicate a negative crosstalk by which CRF_1R activation counteracts OX_1R signaling through G_i in the CRF_1R–OX_1R heteromer. These findings were supported with experiments using label-free DMR technology, which allows measuring G-protein-mediated signaling in living cells. Agonist-induced time–response curves in the absence or presence of pertussis toxin (PTX) or cholera toxin (CTX) were obtained in cells expressing both OX_1R and CRF_1R (Fig. 3A). The maximum response in-
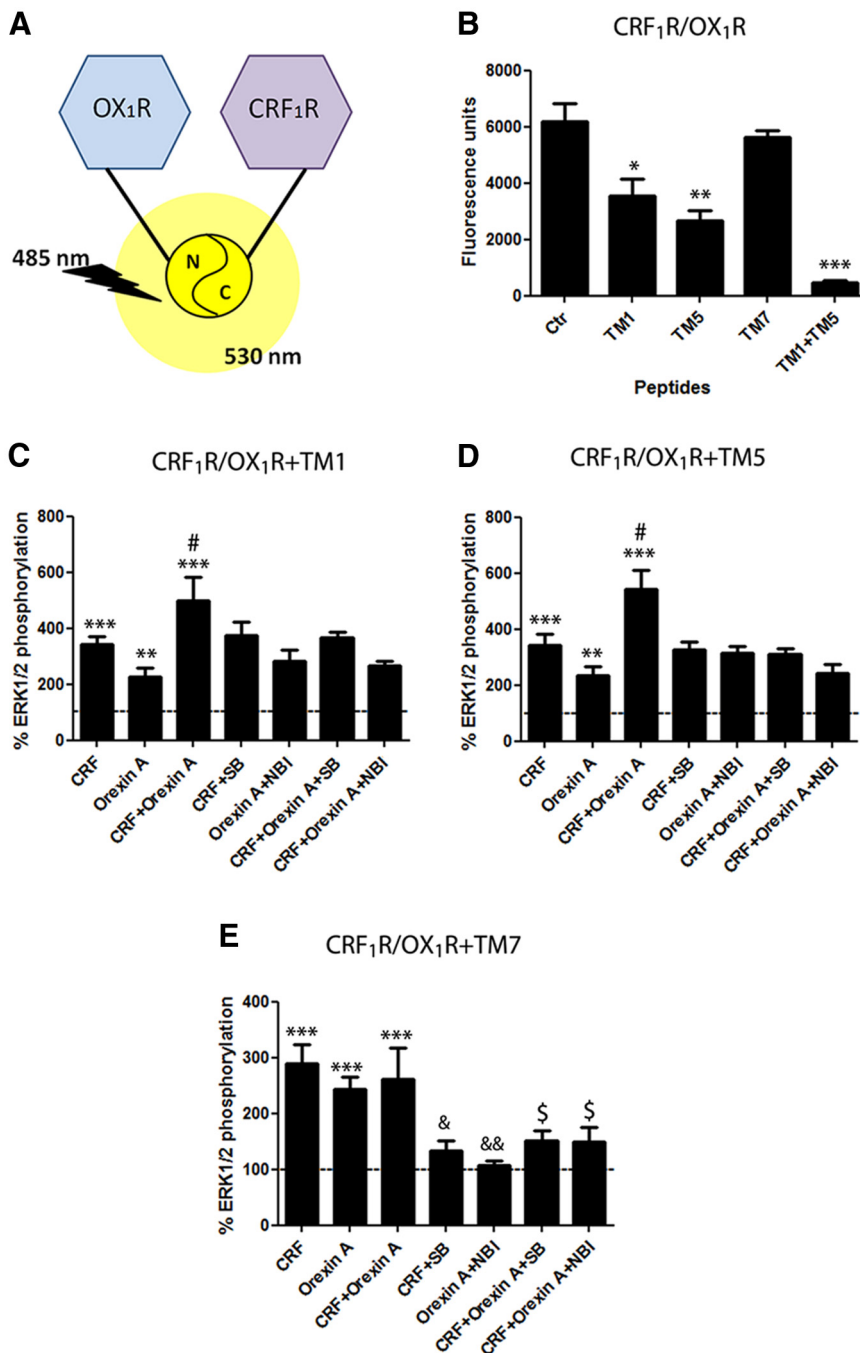
Figure 4. Effect of interfering synthetic peptides on the structure and function of CRF$_1$R–OX$_1$R heteromers. **A**, Scheme showing BiFC. **B**, Disruptive effect of HIV TAT-fused peptides with the amino acid sequences of OX$_1$R TM1, TM5, and TM7 on fluorescence emitted by HEK-293T cells cotransfected with CRF$_1$R–nVenus cDNA (0.6 μM) and OX$_1$R–cVenus cDNA (0.6 μM). Values (fluorescence at 530 nm) are means ± SEMs of six to seven experiments per group. One-way ANOVA followed by Bonferroni's multiple comparison *post hoc* test shows significant differences versus control (Ctr; *$p < 0.05$, **$p < 0.01$, and ***$p < 0.001$). **C–E**, Disruptive effect of HIV TAT-fused peptides on ERK1/2 phosphorylation in HEK-293T cells transfected with CRF$_1$R cDNA (0.3 μg) and OX$_1$R cDNA (0.4 μg) preincubated (60 min) with OX$_1$R TM1, TM5, or TM7 (4 μM), pretreated (20 min) with vehicle, the OX$_1$R antagonist SB334667 (SB; 1 μM), or the CRF$_1$R antagonist NBI27914 (NBI; 1 μM), followed by treatment (7 min) with medium, CRF (100 nM), orexin-A (50 nM), or both. Values are means ± SEMs of five to six experiments expressed as percentage of basal (100%; dotted line). One-way ANOVA followed by Bonferroni's multiple comparison *post hoc* test shows significant differences of agonist treatment versus basal values (**$p < 0.01$ and ***$p < 0.001$), CRF plus orexin-A treatment versus CRF or orexin-A treatment ($^\#p < 0.05$), one agonist plus antagonist versus agonist alone ($^\&p < 0.05$ and $^{\&\&}p < 0.01$), or both agonists plus NBI27914 versus CRF, or both agonists plus SB 334867 versus orexin-A ($^\$p < 0.05$).

duced by orexin-A or CRF (derived from time–response curves) was significantly inhibited with pretreatment with either PTX or CTX (Fig. 3D). Conversely, in cells only expressing CRF$_1$R, the effect of CRF was inhibited by CTX but not with PTX (Fig. 3B), whereas in cells only expressing OX$_1$R, the effect of orexin-A was only inhibited by PTX (Fig. 3C). These results demonstrate that the heteromer can interact simultaneously with both G$_i$- and G$_s$-proteins. Negative crosstalk and cross-antagonism were also observed by DMR. The effect (maximum response) of CRF or orexin-A was inhibited by both NBI27914 and SB334867, and the coactivation with CRF and orexin-A produced a lower response than the one obtained by single activation (Fig. 3E). These results suggest strongly that negative crosstalk and cross-antagonism observed for G-protein-dependent and β-arrestin-dependent signaling pathways constitute biochemical characteristics of CRF$_1$R–OX$_1$R heteromers.

BiFC experiments (Fig. 4A) were performed to check the ability of peptides with the amino acid sequence of OX$_1$R TM domains to destabilize CRF$_1$R–OX$_1$R heteromer, as described recently for the dopamine D$_1$–D$_3$ receptor heteromer (Guitart et al., 2014). HIV TAT peptides fused to OX$_1$R TM1, TM5, and TM7 peptides were used. Significant fluorescence could be detected in HEK-293T cells transfected with CRF$_1$R fused to the N-terminal fragment of YFP Venus (nVenus) and OX$_1$R fused to the C-terminal fragment YFP Venus (cVenus) as a result of YFP Venus reconstitution by CRF$_1$R–OX$_1$R heteromerization. Treatment with OX$_1$R TM1 and TM5 peptides alone or in combination, but not TM7, inhibited YFP Venus reconstitution, and the effect of TM1 plus TM5 was more pronounced than the effect obtained by either peptide alone (Fig. 4B). ERK1/2 phosphorylation crosstalk and cross-antagonism experiments were then performed in cells pretreated with OX$_1$R TM1 (Fig. 4C) or TM5 (Fig. 4D) peptides. Both peptides counteracted the negative crosstalk and cross-antagonism (Fig. 4C,D). Importantly, TM7 peptide, which was not able to alter the structure of CRF$_1$R–OX$_1$R in BiFC experiments, was also ineffective at counteracting the negative crosstalk and cross-antagonism (Fig. 4E). None of the peptides themselves significantly changed signaling from each of the receptors when activated alone with their respective agonists (Fig. 4C–E). These results demonstrate that the negative crosstalk and cross-antagonism depend on the integrity of the quaternary structure of the CRF$_1$R–OX$_1$R heteromer and, therefore, that constitute biochemical characteristics of the heteromer.

Two CRF_1R functional mutants were used to provide some insight about the conformational changes involved in the negative crosstalk between ligands binding to the CRF_1R–OX_1R heteromer: (1) a truncated mutant (CRF_1R433) that lacks a large part of the N-terminal domain and is not able to bind CRF but can still be activated by a small peptide that corresponds to the N-terminal part of CRF (peptide 14b, which binds to the juxtamembrane activating domain of CRF_1R; Devigny et al., 2011); and (2) a receptor that contains a mutation in the third intracellular loop and has enhanced constitutive activity (CRF_1R432). Both mutants were able to form heteromers with OX_1R as detected by BRET experiments without significant differences in $BRET_{max}$ and $BRET_{50}$ with respect to the CRF_1R (Fig. 5A,B). As expected, CRF or orexin-A did not induce ERK1/2 phosphorylation in HEK-293T cells expressing CRF_1R433 alone (Fig. 5C). Orexin-A, but not CRF, was able to signal in cells expressing CRF_1R433–OX_1R heteromers, but orexin-A-induced signaling was not modified by CRF or the CRF_1R antagonist NBI27914 (Fig. 5D,E). Nevertheless, in these cells, peptide 14b promoted ERK1/2 phosphorylation, and a negative crosstalk was observed between orexin-A and peptide 14b (Fig. 5F). These results indicate that an active conformation of the CRF_1R is involved with the negative crosstalk of receptor agonists in the CRF_1R–OX_1R heteromer. This was further corroborated using the CRF_1R432 mutant, which displays high constitutive activity. Single expression of CRF_1R432 showed increased basal ERK1/2 phosphorylation (compared with nontransfected cells), which could not be increased further by CRF (Fig. 5G). The same findings were also obtained in cells expressing CRF_1R432 and OX_1R (Fig. 5H). In addition, orexin-A did not increase MAPK signaling, in agreement with the active conformation of CRF_1R facilitating an allosteric inhibition of the orexin-A signaling (Fig. 5H).

CRF_1R–OX_1R heteromers in the VTA control dendritic dopamine release

In rat VTA slices, orexin-A and CRF promoted ERK1/2 phosphorylation (Fig. 6A), coactivation with orexin-A and CRF showed negative crosstalk, and both the CRF_1R antagonist NBI27914 and the OX_1R antagonist SB334867, which do not modify basal levels by themselves, antagonized the effect of orexin-A and CRF, thus showing cross-antagonism (Fig. 6A). Crosstalk and cross-antagonism disap-
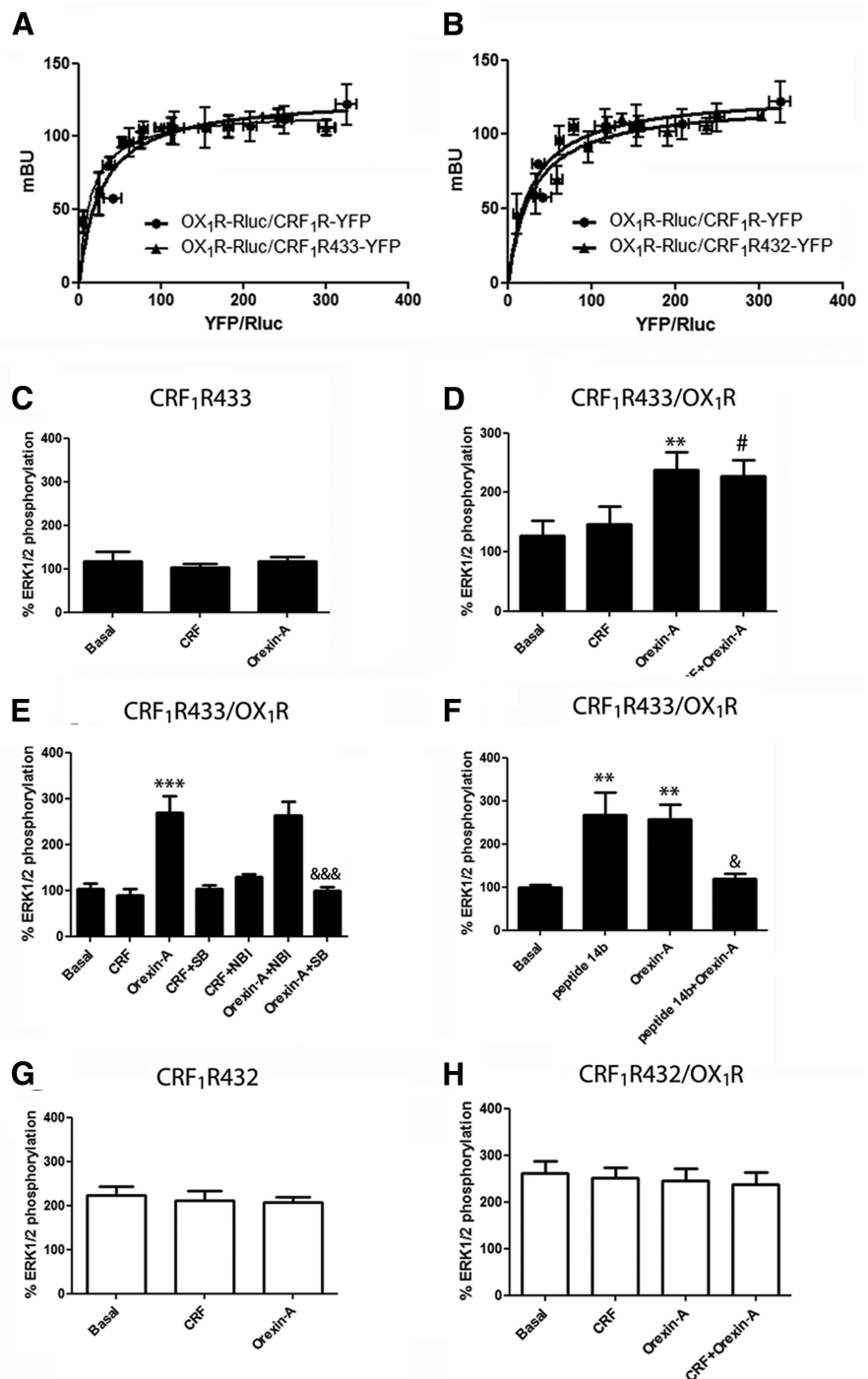

Figure 5. Involvement of the active conformation of CRF_1R with the negative crosstalk of receptor agonists in the CRF_1R–OX_1R heteromer. **A**, **B**, BRET saturation experiments in HEK-293T cells transfected with OX_1R–RLuc cDNA (0.2 μg) and increasing cDNA amounts (0.05–0.5 μg) of CRF_1R–YFP (circles), CRF1R433 mutant (triangles in **A**), or CRF_1R432 mutant (triangles in **B**). BRET is expressed as mBU as a function of 1000 × the ratio between fluorescence of the acceptor (YFP) and Luciferase activity of the donor (RLuc). Values are means ± SEMs of five to six replications of one independent experiment per point. **C–F**, ERK1/2 phosphorylation in HEK-293T cells transfected with CRF1R433 mutant cDNA (0.3 μg; (**B**) alone or transfected with OX_1R cDNA (0.4 μg) pretreated (10 min) with vehicle, the OX_1R antagonist SB334667 (SB; 1 μM), or the CRF_1R antagonist NBI27914 (NBI; 1 μM), followed by treatment (7 min) with CRF (100 nM), orexin-A (50 nM), or both, or with peptide 14b (10 nM; **C–E**). Values are means ± SEMs of five to six experiments per group expressed as percentage of basal (100%). One-way ANOVA followed by Bonferroni's multiple comparison *post hoc* test shows significant differences of single agonist treatment versus basal values (**$p < 0.01$ and ***$p < 0.001$**), CRF plus orexin-A treatment versus CRF or orexin-A treatment ($^{\#}p < 0.05$) or orexin-A plus SB334667 or peptide 14b versus orexin-A alone ($^{\&}p < 0.05$ and $^{\&\&\&}p < 0.001$). **G**, **H**, ERK1/2 phosphorylation in HEK-293T cells transfected with CRF1R432 mutant cDNA (0.3 μg; **F**) alone or transfected with OX_1R (0.4 μg) treated (7 min) with vehicle or with CRF (100 nM), orexin-A (50 nM) or both (**G**). Values are means ± SEMs of five to six experiments per group expressed as percentage of basal values obtained in nontransfected cells (100%).
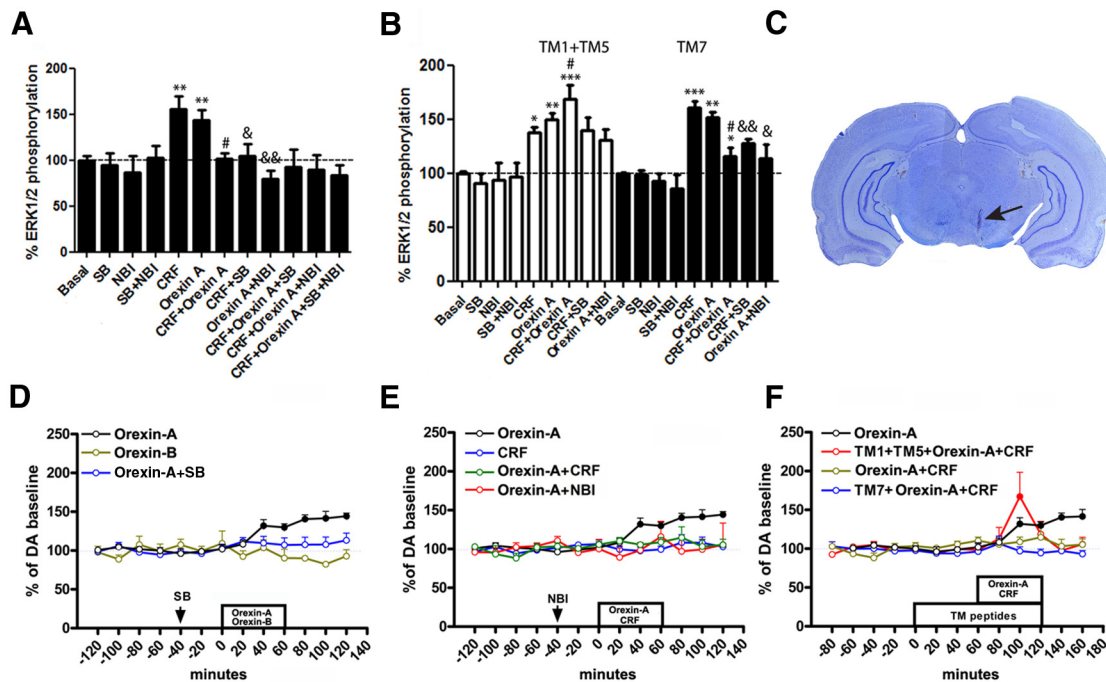
Figure 6. Expression and function of CRF$_1$R–OX$_1$R heteromers in the VTA. *A*, *B*, ERK1/2 phosphorylation in rat VTA slices preincubated (3 h) with vehicle (*A*) or HIV TAT-fused peptides with the amino acid sequences of OX$_1$R TM1 and TM5 (10 μM) or TM7 (20 μM) (30 min) with or without the OX$_1$R antagonist SB334667 (SB; 10 μM) or the CRF$_1$R antagonist NBI27914 (NBI; 10 μM), or both, followed by incubation (10 min) with vehicle, CRF (1 μM), orexin-A (1 μM), or both (*B*). Values are means ± SEMs of five to six experiments per group expressed as percentage of basal values (100%). One-way ANOVA followed by Bonferroni's multiple comparison *post hoc* test shows significant differences of agonist treatment versus basal values (*$p < 0.05$, **$p < 0.01$, and ***$p < 0.001$), CRF plus orexin-A treatment versus CRF or orexin-A treatment ($^\#p < 0.05$), or agonist plus antagonist treatment versus agonist alone ($^\&p < 0.05$ and $^{\&\&}p < 0.01$). *C*, Representative coronal section of a rat brain (5.6 mm posterior from bregma), stained with cresyl violet, showing the track left by the tip of the modified microdialysis probe in the VTA (arrow). *D*, *E*, Dopamine (DA) levels in dialysates sampled from the VTA after slow infusion (1 μl/h) of orexin-A (1 μl, 10 μM), orexin B (1 μl, 10 μM), and/or CRF (1 μl, 10 μM) after previous systemic (intraperitoneal) administration of vehicle, SB334667 (SB; 10 mg/kg; *D*), or NBI27914 (NBI; 10 mg/kg; *E*) or with preinfusion and coinfusion (1 μl/h) of OX$_1$R TM1 plus TM5 (30 μM) or TM7 (60 μM) (*F*). Values are means ± SEMs of 7–10 experiments per group and are expressed as percentage of basal values (average of first 3 values before orexin-A or CRF infusion). A repeated measures ANOVA followed by Bonferroni's multiple comparison *post hoc* test showed significant difference (filled symbols, $p < 0.05$) versus the last basal values before orexin-A or CRF infusion. The same data on the effect of infusion of orexin-A alone are shown in *D–F* for comparison.

peared when VTA slices were treated with the CRF$_1$R–OX$_1$R destabilizing peptides OX$_1$R TM1 plus TM5 (10 μM; Fig. 6*B*), whereas the negative control TM7 peptide (at the same total peptide concentration, 20 μM) was ineffective (Fig. 6*B*), which demonstrates the presence of CRF$_1$R–OX$_1$R heteromers in the VTA.

To investigate the functional role of CRF$_1$R–OX$_1$R heteromers in the VTA, we analyzed dopamine release in the VTA using *in vivo* microdialysis experiments (Fig. 6*C–F*). Dendritic dopamine release by mesencephalic dopaminergic cells resembles that of the terminal regions, possessing a similar uptake mechanism and a finite releasable storage pool (Kita et al., 2009). Furthermore, local dopamine release in the VTA is a correlate of dopaminergic cell firing (Legault and Wise, 1999). Initial attempts to perfuse orexin-A through the dialysis probe (reverse dialysis) were unsuccessful, which included testing of different compositions of ACSF and different dialysis membranes of different materials and different cutoff, as analyzed with mass-spectrometry analysis of *in vitro*-recovered dialysates (data not shown). A specialized probe with an embedded silica infusion port was designed (Fig. 7) that allowed simultaneous constant slow delivery (1 μl/h) of large peptides (ligands and OX$_1$R TM peptides) in the same brain region where the microdialysis probe is sampling the extracellular concentration of dopamine. VTA infusion of orexin-A (10 μM) for 60 min produced dopamine release, which remained elevated >1 h after withdrawal (Fig. 6*D*). The average basal dialysate concentration of dopamine of a total of 121 animals was 2.37 ± 0.15 nM (mean ± SEM). This effect was attrib-

utable to selective activation of OX$_1$R, because it was not reproduced by a 10 μM infusion of the selective OX$_2$R agonist orexin-B (Sakurai et al., 1998; de Lecea et al., 1998) and was counteracted by the previous systemic administration of an effective dose (10 mg/kg, i.p.) of the selective OX$_1$R receptor antagonist SB334867 (Richards et al., 2008; Fig. 6*D*). The infusion of CRF (10 μM) or the systemic administration of an effective dose (10 mg/kg, i.p.) of the CRF$_1$R antagonist NBI27914 did not produce any significant change in the extracellular concentration of dopamine, but both counteracted the effect of orexin-A (Fig. 6*E*), demonstrating the negative crosstalk and cross-antagonism. These results strongly suggest that dendritic VTA dopamine release is under the control of CRF$_1$R–OX$_1$R heteromers. This was further demonstrated using CRF$_1$R–OX$_1$R destabilizing peptides. Infusion of OX$_1$R TM1 (30 μM) plus TM5 (30 μM) peptides but not the control TM7 peptide (at the same total peptide concentration, 60 μM) counteracted the orexin-A–CRF negative crosstalk (Fig. 6*F*). The effect of the TM peptides was not long lasting, probably because of a faster clearance compared with that of the larger and more hydrophilic orexin-A and CRF molecules. These results demonstrate that CRF$_1$R–OX$_1$R heteromers modulate VTA dopamine release.

CRF$_1$R–OX$_1$R heteromers are signaling units that can be modulated by cocaine in transfected cells and the VTA

In cells expressing CRF$_1$R and OX$_1$R, pretreatment for 2 h with 30 μM cocaine completely disrupted the negative crosstalk and
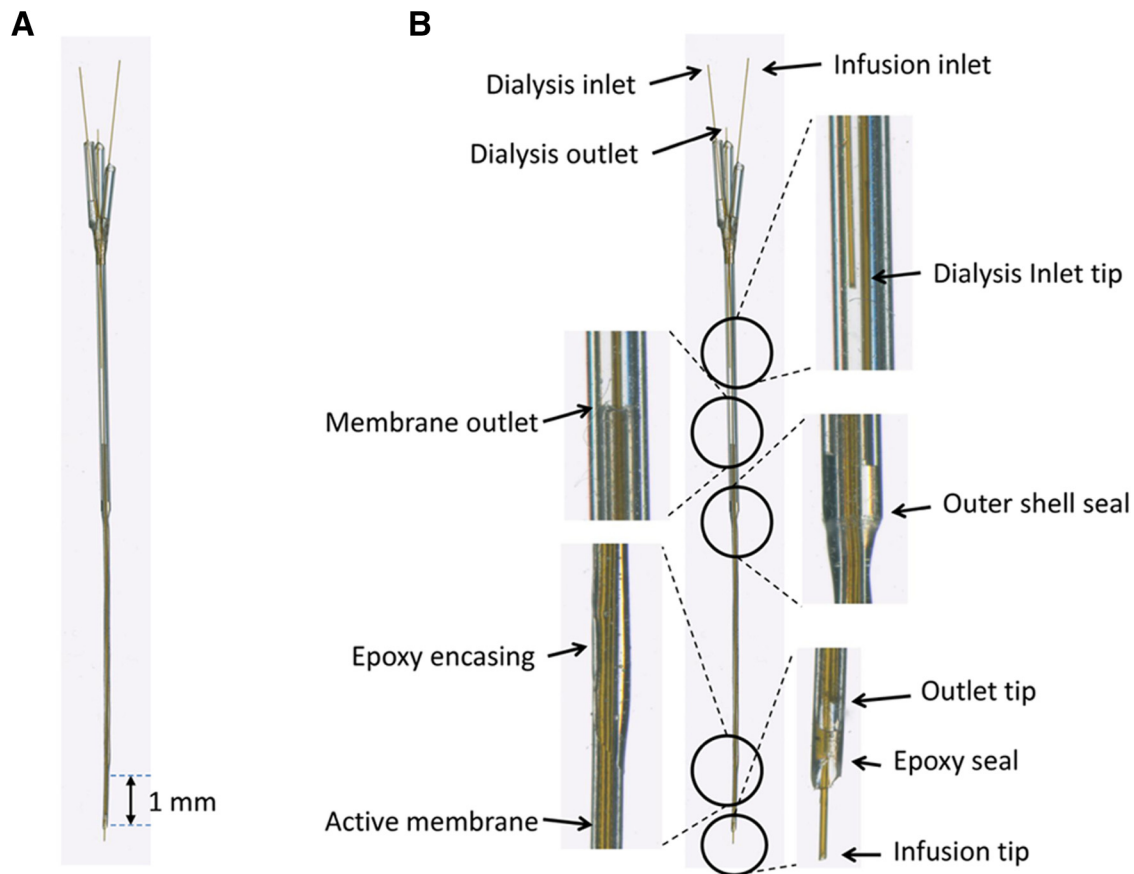
A

B

Figure 7. Microdialysis probe with infusion port. *A*, Magnification showing the length of the dialysis membrane between dotted lines (1 mm). *B*, Amplification of different parts of the probe (on a borosilicate glass model to show inner details). Internal tubing and infusion port are made of fused silica (40 mm internal diameter). The dialysis membrane (AN69) has a 20 kDa molecular weight cutoff. Seals are made of epoxy resin. The design allows the infusing of large peptides in the same brain region being analyzed for extracellular levels of dopamine.

cross-antagonism between CRF_1R and OX_1R ligands on MAPK signaling (Fig. 8A, black, bars) and β-arrestin 2 recruitment (Fig. 8B, black bars) that was seen in the absence of cocaine (Fig. 8 A, B, white bars). Thus, cocaine blocks the allosteric intermolecular interactions in the CRF_1R–OX_1R heteromers that conduce the crosstalk and cross-antagonism between CRF_1R and OX_1R ligands.

We next explored the effect of cocaine in the rat VTA. The extracellular level of cocaine in the rat brain reached after pharmacologically significant doses is estimated to be 15 μM (Pettit et al., 1990). A higher cocaine concentration (100 μM) was then used to allow diffusion into the VTA slices. Cocaine pretreatment for 4 h counteracted the negative crosstalk of orexin-A and CRF on ERK1/2 phosphorylation. Furthermore, cross-antagonism of SB334867 or NBI27914 on ERK1/2 phosphorylation induced by CRF or orexin-A was not observed (Fig. 8C). Therefore, cocaine also disrupts the allosteric interactions within the CRF_1R–OX_1R heteromer in the VTA.

σ_1Rs mediate the disruptive effects of cocaine on CRF_1R–ORX_1R heteromer function

It has been found recently that cocaine can disrupt allosteric interactions between ligands in dopamine D_1–histamine H_3 receptor (H_3R) heteromers by acting on σ_1Rs that oligomerize with the heteromer (Moreno et al., 2014). We explored whether this mechanism could be involved in the disruptive effects of cocaine on CRF_1R–ORX_1R heteromer function. A saturable BRET curve was obtained in HEK-293T cells expressing CRF_1R–RLuc and

increasing concentrations of σ_1R–YFP (Fig. 9A), indicating a direct interaction between σ_1R and CRF_1R. Cocaine produced a significant change in $BRET_{max}$ and $BRET_{50}$ BRET values (Fig. 9A), indicating a cocaine-induced change in the quaternary structure of the σ_1R–CRF_1R oligomers. Conversely, no significant BRET was detected in cells expressing OX_1R–RLuc and σ_1R–YFP in the absence or presence of cocaine (Fig. 9B). These results suggest that σ_1R can interact with CRF_1R–OX_1R heteromers by binding to CRF_1R in the heteromer. The heterotrimeric complex expression was demonstrated with SRET (Fig. 10A; Carriba et al., 2008). In HEK-293T cells expressing a constant amount of OX_1R–RLuc and σ_1R–YFP and increasing amounts of CRF_1R–Cherry, a net SRET saturation curve was obtained (Fig. 10B) with an $SRET_{max}$ of 0.31 $\pm$ 0.01 mSU and a $SRET_{50}$ of 0.08 $\pm$ 0.01. These results provide evidence for the existence of σ_1R–CRF_1R–OX_1R oligomers. Cocaine produced a significant change in $SRET_{max}$ and $SRET_{50}$ values ($SRET_{max}$ of 0.19 $\pm$ 0.03 mSU and a $SRET_{50}$ of 0.056 $\pm$ 0.002), indicating a cocaine-induced change in the quaternary structure of the σ_1R–CRF_1R–OX_1R oligomers. The involvement of σ_1R in the effects of cocaine on CRF_1R–OX_1R heteromers function in the VTA was demonstrated by using selective σ_1R ligands. In VTA slices, pretreatment for 4 h with the σ_1R agonist PRE-084 (Garcés-Ramírez et al., 2011) counteracted the negative crosstalk on ERK1/2 phosphorylation detected during CRF and orexin-A coadministration (Fig. 10C). Moreover, pretreatment with the σ_1R antagonist PD144418 (Akunne et al., 1997) blocked the effect of cocaine, and the negative cross-
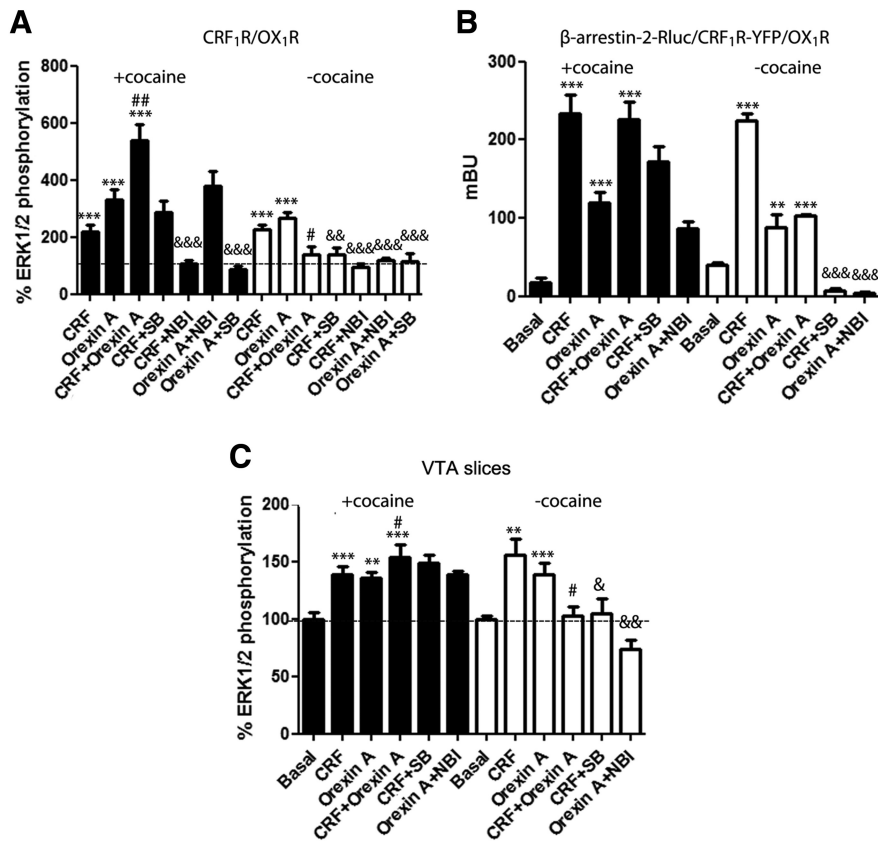
Figure 8. Cocaine-mediated disruption of negative crosstalk and cross-antagonism between CRF$_1$R and OX$_1$R ligands in CRF$_1$R–OX$_1$R heteromers in transfected cells and in the VTA. **A**, ERK1/2 phosphorylation in HEK-293T cells transfected with CRF$_1$R–YFP cDNA (0.3 μg) and OX$_1$R–RLuc cDNA (0.4 μg) pretreated with (black bars) or without (white bars) cocaine (30 μM, 4 h) and (30 min) with vehicle, the OX$_1$R antagonist SB334667 (SB; 1 μM), or the CRF$_1$R antagonist NBI27914 (NBI; 1 μM), followed by treatment (10 min) with CRF (100 nM) or orexin-A (50 nM), or both. Values are means $\pm$ SEMs of six to seven experiments per group expressed as percentage of basal values (100%). One-way ANOVA followed by Bonferroni's multiple comparison *post hoc* test shows significant differences of agonist treatment versus basal values (**$p < 0.01$, ***$p < 0.001$), CRF plus orexin-A treatment versus CRF or orexin-A treatment (##$p < 0.01$), or agonist plus antagonist treatment versus agonist alone (&&&$p < 0.001$). **B**, β-Arrestin 2 recruitment measured by BRET in HEK-293T cells transfected with CRF$_1$R–YFP cDNA (0.3 μg) and OX$_1$R cDNA (0.3 μg) and β-arrestin 2–RLuc cDNA (0.5 μg). Cells were pretreated (2 h) with cocaine (30 μM, black bars) or with medium (white bars) and (10 min) with vehicle, SB334667 (SB; 1 μM), or NBI27914 (NBI; 1 μM), followed by treatment (7 min) with CRF (100 nM), orexin-A (50 nM), or both. Values are means $\pm$ SEMs of five to six experiments per group. One-way ANOVA followed by Bonferroni's multiple comparison *post hoc* test shows significant differences of agonist treatment versus basal (**$p < 0.01$ and ***$p < 0.001$) or agonist plus antagonist treatment versus agonist alone (&&&$p < 0.001$). **C**, ERK1/2 phosphorylation in rat VTA slices preincubated (4 h) with cocaine (100 μM, black bars) or with vehicle (white bars) and (30 min) with vehicle, SB334667 (SB; 10 μM), or NBI27914 (NBI; 10 μM), followed by treatment (10 min) with CRF (1 μM), orexin-A (1 μM) or both. Values are means $\pm$ SEMs of five to six experiments per group expressed as percentage of basal values (100%). One-way ANOVA followed by Bonferroni's multiple comparison *post hoc* test shows significant differences of agonist treatment versus basal values (**$p < 0.01$ and ***$p < 0.001$), CRF plus orexin-A treatment versus CRF or orexin-A treatment (#$p < 0.05$) or agonist plus antagonist treatment versus agonist alone (&$p < 0.05$ and &&$p < 0.01$).

talk between CRF and orexin-A was still present with preincubation of cocaine and PD144418 (Fig. 10D).

Cocaine exerts its stimulant effects predominantly by its ability to block the dopamine transporter (DAT; Kita et al., 2009). To dissect the σ_1R effects in microdialysis experiments, we used the selective σ_1R agonist PRE-084, which reproduced the effects of cocaine in the *in vitro* experiments and has very low affinity for DAT (Garcés-Ramírez et al., 2011). Direct perfusion of the σ_1R agonist PRE-084 (100 μM) through the microdialysis probe did not modify the extracellular concentration of dopamine (Fig. 10F) but counteracted the negative crosstalk between orexin-A and CRF. Thus, in the presence of PRE-084, orexin-A plus CRF produced an increase in extracellular dopamine that was larger than the one induced by orexin-A alone (Fig. 10E). In fact, in the

presence of PRE-084, orexin-A was more effective, particularly during the first two samples (40 min) after its infusion. Interestingly, CRF, which was ineffective by itself, also produced a prolonged significant elevation of extracellular dopamine during perfusion with the σ_1R agonist (Fig. 10F). These results match with the *in vitro* experiments and indicate the existence of a negative crosstalk between orexin-A and CRF, which is counteracted by σ_1R activation. These striking results are in total agreement with σ_1R–CRF$_1$R–OX$_1$R oligomers modulating VTA dopamine release.

We then studied whether one single administration of cocaine (15 mg/kg) could also reproduce the effects of the acute perfusion of the σ_1R agonist PRE-084 attributable to a long-term disruption of the allosteric interactions in the CRF$_1$R–OX$_1$R heteromer, as demonstrated recently for σ_1R–D$_1$R–H$_3$R oligomers (Moreno et al., 2014). In fact, a significant elevation in the extracellular concentration of VTA dopamine was observed after infusion of CRF or coinfusion of orexin-A and CRF (Fig. 10G).

Discussion

Class B GPCR CRF$_1$R has been shown previously to homomerize (Milan-Lobo et al., 2009) and also heteromerize with the class A GPCRs for vasopressin and its non-mammalian vertebrate homolog vasotocin in transfected cells (Mikhailova et al., 2007; Murat et al., 2012). Similarly, evidence has been reported for OX$_1$R homomerization and heteromerization in artificial cell systems (Ellis et al., 2006; Jäntti et al., 2014). However, although colocalized in the VTA, CRF$_1$R–OX$_1$R heteromerization has not been described, and, in fact, it has been argued that independent actions of CRF and orexin-A in the VTA are involved in reinstatement of cocaine seeking (Wang et al., 2009). In the present study, we demonstrate the existence of functional CRF$_1$R–OX$_1$R heteromers in transfected cells and the VTA, in which they exert a significant functional control of dopaminergic cells. By means of allosteric interactions within the CRF$_1$R–OX$_1$R heteromer, CRF and orexin-A antagonize each other's ability to signal and promote VTA dendritic dopamine release, indicating that this heteromer should play a significant role under stress conditions, during concomitant CRF and orexin-A VTA release. Additional important findings were the evidence for oligomerization of σ_1R with the CRF$_1$R–OX$_1$R heteromer and the ability of σ_1R agonists, including cocaine, to modify the quaternary structure of the heteromer to block the functional allosteric interactions between orexin-A and CRF within the heteromer.

Molecular interactions between CRF$_1$R and OX$_1$R were demonstrated in HEK-293T cells by using different approaches,
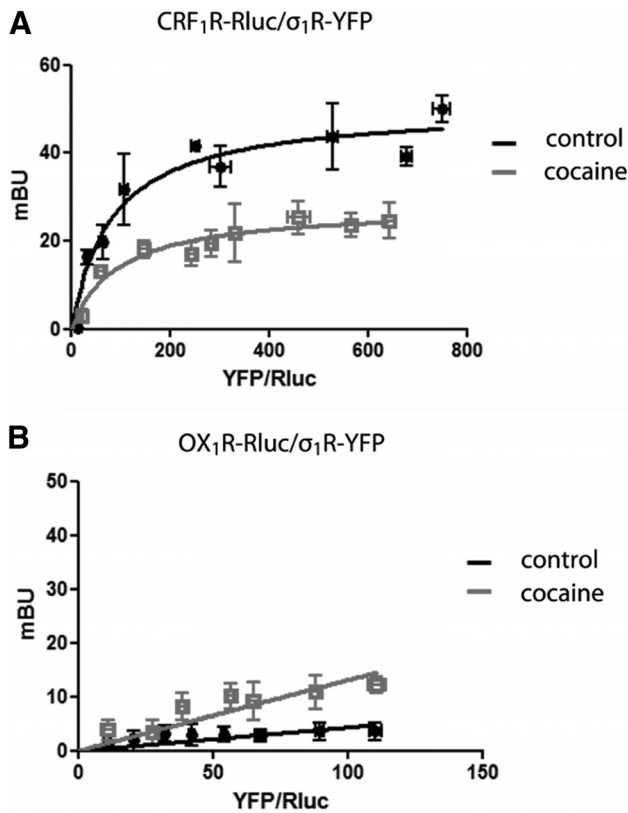
Figure 9. Interaction of σ_1R with CRF$_1$R. BRET saturation experiments in HEK-293T cells transfected with CRF$_1$R-RLuc cDNA (0.3 μg; **A**) or OX$_1$R–RLuc cDNA (0.4 μg; **B**) with increasing amounts of σ_1R–YFP cDNA (0.06 – 0.7 μg), in the absence (black curves) or presence (red curves) of cocaine (30 μM). BRET, expressed as mBU, is given as a function of 1000 × the ratio between the fluorescence of the acceptor (YFP) and the Luciferase activity of the donor (RLuc). Values are means ± SEMs of five to six experiments.

which included BRET, fluorescence complementation, and PLA, but also additional demonstration came from results of signaling experiments indicating the expression of CRF$_1$R–OX$_1$R heteromers at the membrane level. To our knowledge, the ability of an antagonist of one receptor to block the agonist-mediated signaling of another receptor has only been reported in the frame of receptor heteromerization (Ferré et al., 2014). Also, the ability of orexin-A to induce an interaction between β-arrestin 2–RLuc and CRF$_1$R–YFP indicates recruitment of β-arrestin 2 to the CRF$_1$R–OX$_1$R heteromer. Moreover, the surprising ability of PTX to counteract G$_s$-mediated CRF$_1$R signaling and that of CTX to block G$_i$-mediated OX$_1$R signaling indicate that the CRF$_1$R–OX$_1$R heteromer can interact simultaneously with both G$_i$ and G$_s$ proteins showing an interdependence of G$_i$ and G$_s$ protein function in the heteromer.

Demonstration of unique biochemical properties of a receptor heteromer requires their dependence on the structural integrity of the heteromer (Ferré et al., 2009, 2014), which can be destabilized, for instance, by interfering synthetic peptides with the amino acid sequence corresponding to some TM or intracellular domains of one of the protomers (Azdad et al., 2009; He et al., 2011; Guitart et al., 2014). BRET and complementation experiments in transfected cells demonstrated that specific OX$_1$R TM peptides and σ_1R agonists significantly modify the quaternary structure of the CRF$_1$R–OX$_1$R heteromer. Therefore, both were used as tools to interrogate the CRF$_1$R–OX$_1$R heteromer function. In fact, both OX$_1$R TM peptides and σ_1R agonists sig-

nificantly counteracted negative crosstalk and cross-antagonism of CRF$_1$R and OX$_1$R ligands, demonstrating that they constitute biochemical properties of the CRF$_1$R–OX$_1$R heteromer. The application of the same tools *in situ* and *in vivo*, in VTA slices and in microdialysis experiments, further demonstrated the presence of CRF$_1$R–OX$_1$R heteromers in the VTA. The very different quantitative effect of OX$_1$R TM peptides versus σ_1R agonists observed *in vivo*, with a respective transient versus long-lasting (apparently irreversible) destabilization of CRF$_1$R–OX$_1$R-heteromer function, should be related to the different molecular mechanisms and different modifications of the quaternary structure of the heteromer involved. Particularly significant will be the elucidation of the apparently irreversible effect of σ_1R agonists, such as cocaine.

An important amount of experimental data demonstrates the involvement of σ_1R in many pharmacologic, including rewarding, effects of cocaine (Maurice and Su, 2009; Robson et al., 2012). Recent studies describe a role of oligomerization of σ_1R with D$_1$R or D$_2$R in the acute psychostimulants effects of cocaine (Navarro et al., 2010, 2013) and with voltage-gated Kv1.2 potassium channels in long-lasting behavioral responses (Kourrich et al., 2013). Also, oligomerization of σ_1R, D$_1$R, and H$_3$Rs (σ_1R–D$_1$R–H$_3$R heteromers) has been involved in the neurotoxic effects of cocaine (Moreno et al., 2014). Interestingly, when comparing the effects of cocaine binding with either σ_1R-D$_1$R–H$_3$R or σ_1R–CRF$_1$R–OX$_1$R oligomers, a common mechanism emerges, the loss of the allosteric interactions between ligands in the heteromer.

The present results strongly suggest that CRF$_1$R–OX$_1$R heteromers localized in the VTA convey the previously established significant control of dopaminergic cell function by CRF and orexin-A in cocaine-treated animals. The counteraction of the negative crosstalk between orexin-A and CRF in the VTA by the simultaneous application of the σ_1R agonist PRE-084 or by the previous administration of cocaine provides a mechanism by which CRF can only induce VTA dendritic dopamine release in animals exposed previously to cocaine (Wang et al., 2005). Under these conditions, CRF$_1$R-mediated signaling is not inhibited by a tonic activation of OX$_1$R by endogenous orexin-A. Counteraction of the allosteric interactions between agonists in the CRF$_1$R–OX$_1$R heteromer can also explain the apparent CRF-independent ability of orexin-A to release dopamine in the VTA and to induce cocaine seeking (Wang et al., 2009). Remarkably, in the present study, cocaine produced a modification of CRF$_1$R–OX$_1$R heteromer function that was observed 24 h after one single systemic administration. Very similar findings were reported recently for σ_1R–D$_1$R–H$_3$R oligomers, in which the ability of H$_3$R ligands to modulate D$_1$R-mediated signaling was also disrupted 24 h after one single systemic administration of cocaine (Moreno et al., 2014). Therefore, one single administration could explain some effects of cocaine attributed previously to its repeated administration.

Of the many new questions this study raises is the identification of the precise localization of CRF$_1$R–OX$_1$R heteromers in the VTA. Both receptors are potentially colocalized in dopaminergic cells and their glutamatergic afferents Borgland et al., 2010), in which CRF$_1$R–OX$_1$R heteromers could directly or indirectly control the extracellular levels of dopamine in the VTA. Second, our data indicate that, under basal conditions, the effects of CRF and orexin-A in the VTA are interdependent and mediated by CRF$_1$R–OX$_1$R heteromers, but they also suggest that endogenous σ_1R ligands should be able to act as cocaine and therefore promote independent effects of CRF and orexin-A. Those ligands and the conditions under which they are produced in the VTA
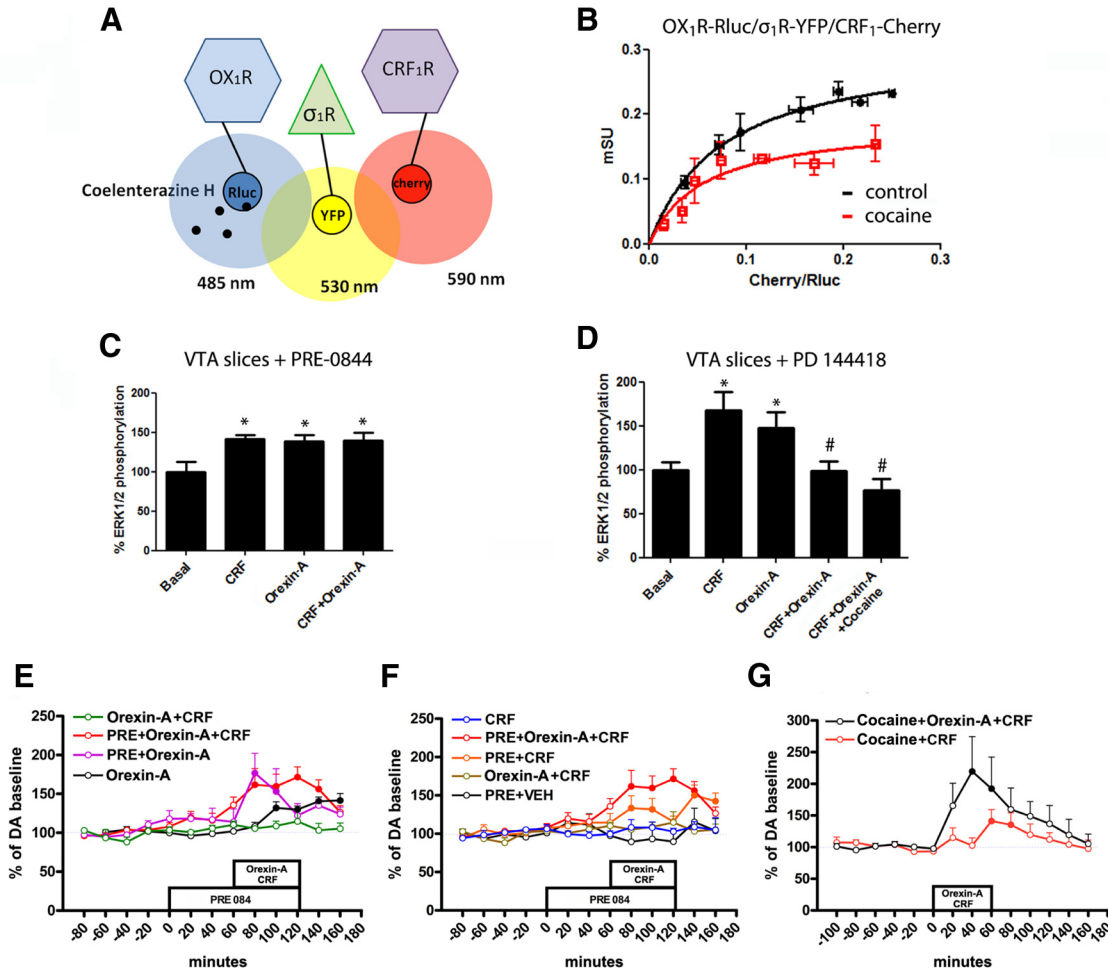
Figure 10. Involvement of σ_1R in the disruptive effect of cocaine on CRF$_1$R–OX$_1$R heteromer function. **A**, Scheme showing SRET (see Results). **B**, SRET saturation experiments in HEK-293T cells expressing a constant amount of OX$_1$R–RLuc cDNA (0.2 μg of cDNA transfected) and σ_1R–YFP cDNA (0.3 μg) and increasing amounts of CRF$_1$R–Cherry cDNA (0.05–0.6 μg) in controls (black curve) or cocaine-treated (30 min, 30 μM; red curve) cells. SRET, expressed as mSU, is given as a function of the ratio between the fluorescence of the acceptor (Cherry) and the Luciferase activity of the donor (RLuc). Values are means $\pm$ SEMs of seven to eight replications of one independent experiment per point. **C**, ERK1/2 phosphorylation in rat VTA slices preincubated (4 h) with the σ_1R agonist PRE-084 (1 μM), followed by treatment (10 min) with CRF (1 μM), orexin-A (1 μM), or both. **D**, ERK1/2 phosphorylation in rat VTA slices preincubated (4 h) with the σ_1R antagonist PD144418 (1 μM), with or without cocaine (100 μM), followed by treatment (10 min) with CRF (1 μM), orexin-A (1 μM), or both. In **C** and **D**, values are means $\pm$ SEMs of five to six experiments per group expressed as percentage of basal values (100%). One-way ANOVA followed by Bonferroni's multiple comparison *post hoc* test showed significant differences versus basal (*$p < 0.05$) and CRF plus orexin-A treatment versus CRF or orexin-A treatment ([#]$p < 0.05$). **E–G**, Dopamine (DA) levels in dialysates sampled from the VTA after slow infusion (1 μl/h) of orexin-A (1 μM, 10 μM) and/or CRF (1 μl, 10 μM) with preinfusion and coinfusion of the σ_1R agonist PRE-084 (PRE; 100 μM) or previous systemic (intraperitoneal) administration of cocaine (COC; 15 mg/kg; 24 h before the microdialysis experiment). Values are means $\pm$ SEMs of 7–10 experiments per group and are expressed as percentage of basal values (average of first 3 values before orexin-A or CRF infusion). A repeated-measures ANOVA (including only the basal value before orexin-A or CRF infusion) followed by Bonferroni's multiple comparison *post hoc* test showed significant differences (filled symbols, $p < 0.05$) versus the last basal values before orexin-A or CRF infusion. Data on the effect of infusion of orexin-A alone in **E** are the same shown in Figure 6D–F.

still need to be determined. Third is to understand the potential changes in σ_1R–CRF$_1$R–OX$_1$R oligomers in acute versus long-term exposure to cocaine. It has been shown that repeated cocaine exposure increases the levels of σ_1R in the brain (Robson et al., 2012), and cocaine-mediated upregulation of striatal σ_1R has been reported to increase the presence of σ_1–Kv1.2 oligomers at the plasma membrane, which has been suggested to be involved in sensitization to its psychostimulants effects (Kourrich et al., 2013). Therefore, upregulation of σ_1R in the VTA could increase the proportion of σ_1R–CRF$_1$R–OX$_1$R oligomers, leading to more profound cocaine-induced changes in the control of VTA dendritic dopamine release by CRF and orexin-A. Those changes could explain the CRF$_1$R-dependent augmented cocaine seeking in response to stress or CRF delivered into the VTA after long-access self-administration (Blacktop et al., 2011). Altogether, the

present study demonstrates a significant functional and pharmacological role of σ_1R in the modulation of CRF$_1$R–OX$_1$R heteromers during physiological conditions and under conditions of acute cocaine administration and withdrawal. Addressing the study of σ_1R–CRF$_1$R–OX$_1$R oligomers in animal models of psychostimulant abuse should provide significant additional information that would support their role as new therapeutic targets.

References

Akunne HC, Whetzel SZ, Wiley JN, Corbin AE, Ninteman FW, Tecle H, Pei Y, Pugsley TA, Heffner TG (1997) The pharmacology of the novel and selective sigma ligand, PD 144418. Neuropharmacology 36:51–62. CrossRef Medline

Azdad K, Gall D, Woods AS, Ledent C, Ferré S, Schiffmann SN (2009) Dopamine D2 and adenosine A2A receptors regulate NMDA-mediated excitation in accum-

bens neurons through A2A-D2 receptor heteromerization. Neuropsychopharmacology 34:972–986. CrossRef Medline

Blacktop JM, Seubert C, Baker DA, Ferda N, Lee G, Graf EN, Mantsch JR (2011) Augmented cocaine seeking in response to stress or CRF delivered into the ventral tegmental area following long-access self-administration is mediated by CRF receptor type 1 but not CRF receptor type 2. J Neurosci 31:11396–11403. CrossRef Medline

Borgland SL, Ungless MA, Bonci A (2010) Convergent actions of orexin/hypocretin and CRF on dopamine neurons: emerging players in addiction. Brain Res 1314:139–144. CrossRef Medline

Boutrel B, Kenny PJ, Specio SE, Martin-Fardon R, Markou A, Koob GF, de Lecea L (2005) Role for hypocretin in mediating stress-induced reinstatement of cocaine-seeking behavior. Proc Natl Acad Sci U S A 102:19168–19173. CrossRef Medline

Carriba P, Navarro G, Ciruela F, Ferré S, Casadó V, Agnati L, Cortés A, Mallol J, Fuxe K, Canela EI, Lluís C, Franco R (2008) Detection of heteromerization of more than two proteins by sequential BRET-FRET. Nat Methods 5:727–233. CrossRef Medline

de Lecea L, Kilduff TS, Peyron C, Gao X, Foye PE, Danielson PE, Fukuhara C, Battenberg EL, Gautvik VT, Bartlett FS 2nd, Frankel WN, van den Pol AN, Bloom FE, Gautvik KM, Sutcliffe JG (1998) The hypocretins: hypothalamus-specific peptides with neuroexcitatory activity. Proc Natl Acad Sci U S A 95:322–327. CrossRef Medline

Devigny C, Perez-Balderas F, Hoogeland B, Cuboni S, Wachtel R, Mauch CP, Webb KJ, Deussing JM, Hausch F (2011) Biomimetic screening of class-B G protein-coupled. J Am Chem Soc 133:8927–8933. CrossRef Medline

Ellis J, Pediani JD, Canals M, Milasta S, Milligan G (2006) Orexin-1 receptor-cannabinoid CB1 receptor heterodimerization results in both ligand-dependent and -independent coordinated alterations of receptor localization and function. J Biol Chem 281:38812–38824. CrossRef Medline

Ferré S, Baler R, Bouvier M, Caron MG, Devi LA, Durroux T, Fuxe K, George SR, Javitch JA, Lohse MJ, Mackie K, Milligan G, Pfleger KD, Pin JP, Volkow ND, Waldhoer M, Woods AS, Franco R (2009) Building a new conceptual framework for receptor heteromers. Nat Chem Biol 5:131–134. CrossRef Medline

Ferré S, Casadó V, Devi LA, Filizola M, Jockers R, Lohse MJ, Milligan G, Pin JP, Guitart X (2014) Protein-coupled receptor oligomerization revisited: functional and pharmacological perspectives. Pharmacol Rev 66:413–434. CrossRef Medline

Garcés-Ramírez L, Green JL, Hiranita T, Kopajtic TA, Mereu M, Thomas AM, Mesangeau C, Narayanan S, McCurdy CR, Katz JL, Tanda G (2011) Sigma receptor agonists: receptor binding and effects on mesolimbic dopamine neurotransmission assessed by microdialysis. Biol Psychiatry 69:208–217. CrossRef Medline

Guitart X, Navarro G, Moreno E, Yano H, Cai NS, Sánchez-Soto M, Kumar-Barodia S, Naidu YT, Mallol J, Cortés A, Lluís C, Canela EI, Casadó V, McCormick PJ, Ferré S (2014) Functional selectivity of allosteric interactions within GPCR oligomers: the dopamine D1–D3 receptor heterotetramer. Mol Pharmacol 86:417–429. CrossRef Medline

He SQ, Zhang ZN, Guan JS, Liu HR, Zhao B, Wang HB, Li Q, Yang H, Luo J, Li ZY, Wang Q, Lu YJ, Bao L, Zhang X (2011) Facilitation of μ-opioid receptor activity by preventing δ-opioid receptor-mediated codegradation. Neuron 69:120–131. CrossRef Medline

Jäntti MH, Mandrika I, Kukkonen JP (2014) Human orexin/hypocretin receptors form constitutive homo- and heteromeric complexes with each other and with human CB1 cannabinoid receptors. Biochem Biophys Res Commun 445:486–490. CrossRef Medline

Kita JM, Kile BM, Parker LE, Wightman RM (2009) In vivo measurement of somatodendritic release of dopamine in the ventral tegmental area. Synapse 63:951–960. CrossRef Medline

Kourrich S, Hayashi T, Chuang JY, Tsai SY, Su TP, Bonci A (2013) Dynamic interaction between sigma-1 receptor and Kv1.2 shapes neuronal and behavioral responses to cocaine. Cell 152:236–247. CrossRef Medline

Kovacs JJ, Hara MR, Davenport CL, Kim J, Lefkowitz RJ (2009) Arrestin development: emerging roles for beta-arrestins in developmental signaling pathways. Dev Cell 17:443–458. CrossRef Medline

Legault M, Wise RA (1999) Injections of N-methyl-D-aspartate into the ventral hippocampus increase extracellular dopamine in the ventral tegmental area and nucleus accumbens. Synapse 31:241–249. CrossRef Medline

Lodge DJ, Grace AA (2005) Acute and chronic corticotropin-releasing factor 1 receptor blockade inhibits cocaine-induced dopamine release: correlation with dopamine neuron activity. J Pharmacol Exp Ther 314:201–206. CrossRef Medline

Lu L, Liu Z, Huang M, Zhang Z (2003) Dopamine-dependent responses to cocaine depend on corticotropin-releasing factor receptor subtypes. J Neurochem 84:1378–1386. CrossRef Medline

Mahler SV, Moorman DE, Smith RJ, James MH, Aston-Jones G (2014) Motivational activation: a unifying hypothesis of orexin/hypocretin function. Nat Neurosci 17:1298–1303. CrossRef Medline

Maurice T, Su TP (2009) The pharmacology of sigma-1 receptors. Pharmacol Ther 124:195–206. CrossRef Medline

Mikhailova MV, Mayeux PR, Jurkevich A, Kuenzel WJ, Madison F, Periasamy A, Chen Y, Cornett LE (2007) Heterooligomerization between vasotocin and corticotropin-releasing hormone (CRH) receptors augments CRH-stimulated 3′,5′-cyclic adenosine monophosphate production. Mol Endocrinol 21:2178–2188. CrossRef Medline

Milan-Lobo L, Gsandtner I, Gaubitzer E, Rünzler D, Buchmayer F, Köhler G, Bonci A, Freissmuth M, Sitte HH (2009) Subtype-specific differences in corticotropin-releasing factor receptor complexes detected by fluorescence spectroscopy. Mol Pharmacol 76:1196–1210. CrossRef Medline

Moreno E, Moreno-Delgado D, Navarro G, Hoffmann HM, Fuentes S, Rosell-Vilar S, Gasperini P, Rodríguez-Ruiz M, Medrano M, Mallol J, Cortés A, Casadó V, Lluís C, Ferré S, Ortiz J, Canela E, McCormick PJ (2014) Cocaine disrupts histamine H3 receptor modulation of dopamine D1 receptor signaling: σ1-D1-H3 receptor complexes as key targets for reducing cocaine's effects. J Neurosci 34:3545–3558. CrossRef Medline

Murat B, Devost D, Andrés M, Mion J, Boulay V, Corbani M, Zingg HH, Guillon G (2012) V1b and CRHR1 receptor heterodimerization mediates synergistic biological actions of vasopressin and CRH. Mol Endocrinol 26:502–520. CrossRef Medline

Navarro G, Moreno E, Aymerich M, Marcellino D, McCormick PJ, Mallol J, Cortés A, Casadó V, Canela EI, Ortiz J, Fuxe K, Lluís C, Ferré S, Franco R (2010) Direct involvement of sigma-1 receptors in the dopamine D1 receptor-mediated effects of cocaine. Proc Natl Acad Sci U S A 107:18676–18681. CrossRef Medline

Navarro G, Moreno E, Bonaventura J, Brugarolas M, Farré D, Aguinaga D, Mallol J, Cortés A, Casadó V, Lluís C, Ferre S, Franco R, Canela E, McCormick PJ (2013) Cocaine inhibits dopamine D2 receptor signaling via sigma-1-D2 receptor heteromers. PLoS One 8:e61245. CrossRef Medline

Pettit HO, Pan HT, Parsons LH, Justice JB Jr (1990) Extracellular concentrations of cocaine and dopamine are enhanced during chronic cocaine administration. J Neurochem 55:798–804. CrossRef Medline

Richards JK, Simms JA, Steensland P, Taha SA, Borgland SL, Bonci A, Bartlett SE (2008) Inhibition of orexin-1/hypocretin-1 receptors inhibits yohimbine-induced reinstatement of ethanol and sucrose seeking in Long-Evans rats. Psychopharmacology 199:109–117. CrossRef Medline

Robson MJ, Noorbakhsh B, Seminerio MJ, Matsumoto RR (2012) Sigma-1 receptors: potential targets for the treatment of substance abuse. Curr Pharm Des 18:902–919. CrossRef Medline

Rodaros D, Caruana DA, Amir S, Stewart J (2007) Corticotropin-releasing factor projections from limbic forebrain and paraventricular nucleus of the hypothalamus to the region of the ventral tegmental area. Neuroscience 150:8–13. CrossRef Medline

Saal D, Dong Y, Bonci A, Malenka RC (2003) Drugs of abuse and stress trigger a common synaptic adaptation in dopamine neurons. Neuron 37:577–582. CrossRef Medline

Sakurai T (2014) The role of orexin in motivated behaviours. Nat Rev Neurosci 15:719–731. CrossRef Medline

Sakurai T, Amemiya A, Ishii M, Matsuzaki I, Chemelli RM, Tanaka H, Williams SC, Richardson JA, Kozlowski GP, Wilson S, Arch JR, Buckingham RE, Haynes AC, Carr SA, Annan RS, McNulty DE, Liu WS, Terrett JA, Elshourbagy NA, Bergsma DJ, Yanagisawa M (1998) Orexins and orexin receptors: a family of hypothalamic neuropeptides and G protein-coupled receptors that regulate feeding behavior. Cell 92:573–585. CrossRef Medline

Sarnyai Z, Shaham Y, Heinrichs SC (2001) The role of corticotropin-releasing factor in drug addiction. Pharmacol Rev 53:209–243. Medline

Schwarze SR, Ho A, Vocero-Akbani A, Dowdy SF (1999) In vivo protein transduction: delivery of a biologically active protein into the mouse. Science 285:1569–1572. CrossRef Medline

Shaham Y, Erb S, Leung S, Buczek Y, Stewart J (1998) CP-154,526, a selective, non-peptide antagonist of the corticotropin-releasing factor1 receptor attenuates stress-induced relapse to drug seeking in cocaine- and heroin-trained rats. Psychopharmacology 137:184–190. CrossRef Medline

Ungless MA, Singh V, Crowder TL, Yaka R, Ron D, Bonci A (2003) Corticotropin-releasing factor requires CRF binding protein to potentiate NMDA receptors via CRF receptor 2 in dopamine neurons. Neuron 39: 401–407. CrossRef Medline

Wang B, Shaham Y, Zitzman D, Azari S, Wise RA, You ZB (2005) Cocaine experience establishes control of midbrain glutamate and dopamine by corticotropin-releasing factor: a role in stress-induced relapse to drug seeking. J Neurosci 25:5389–5396. CrossRef Medline

Wang B, You ZB, Rice KC, Wise RA (2007) Stress-induced relapse to cocaine seeking: roles for the CRF(2) receptor and CRF-binding protein in the ventral tegmental area of the rat. Psychopharmacology 193:283–294. CrossRef Medline

Wang B, You ZB, Wise RA (2009) Reinstatement of cocaine seeking by hypocretin (orexin) in the ventral tegmental area: independence from the local corticotropin-releasing factor network. Biol Psychiatry 65:857–862. CrossRef Medline